UNIVERSITAT POLITÈCNICA DE VALÈNCIA

UNIVERSITAT POLITÈCNICA DE VALÈNCIA

School of Industrial Engineering

Analysis of the combustion process in a compression engine fueled with oxymethylene ether (e-fules) by means of CFD

Master's Thesis

Master's Degree in Industrial Engineering

AUTHOR: Blondeel, Dean

Tutor: Bracho León, Gabriela Cristina

ACADEMIC YEAR: 2022/2023

UNIVERSITAT POLITÈCNICA DE VALÈNCIA

ESCOLA TÈCNICA SUPERIOR ENGINYERIA INDUSTRIAL VALÈNCIA

Analysis of the combustion process in a compression engine fueled with oxymethylene ether (e-fuels) by means of CFD

Supervisor: Gabriela Bracho Leon

Co-supervisor:
Cassio Spohr Fernandes

Master's Thesis submitted to obtain the degree of Master of Science in Engineering Technology: *electro-mechanics*

Academic year 2022-2023

Acknowledgement

This thesis was very educational since a lot of this subject matter I have not been in contact with before, I thought this was very enlightening. Next to enlightening it also was challenging as any master thesis is but I am walking away from this thesis with a lot of new acquired knowledge which I will be able to use in the work field as an Industrial engineer. Although challenging, I was lucky to have the necessary support from every side.

Firstly, I would like to take the opportunity to express my gratitude to my supervisor Gabriela Bracho Leon who would always assist my whenever I had questions and to check my progress. I would also like to thank my co-supervisor Cássio Spohr Fernandes which was ready to assist me when I had questions anytime, for checking on the progress and giving me the necessary push when I ran in to problems.

Secondly, I would like to thank my parents and family for the support and guidance. They were always there when I needed them.

And last but not least, I would like to thank all my friends I have made on Erasmus exchange for the necessary support and motivation when it comes to school. And for the much-needed relaxation as an outlet.

Keywords: Sustainable fuels; e-fuels, combustion process; pollutant emissions reduction; CFD

Abstract

In today's day and age, it is important to discontinue our reliance on fossil fuels. More and more there is being searched for alternative renewable energy. This trend has also been taking place in the vehicle industry, more and more people are looking for an environmentally friendly transport method. As a result, this study makes it very interesting for the future to completely move away from polluting combustion engines on diesel. The renewable fuel under consideration is Oxymethylether (OME_3). In this paper the difference in properties between this e-fuel and diesel are assessed while using oxy-fuel combustion concept to avoid the formation of NOx in the exhaust gases. The properties are analysed by integrating three different comparisons, a comparison where the number of injector nozzle orifices is changed while keeping iso-energy conditions, a comparison under Iso-lambda and Iso-energy conditions. From these two comparisons the results are analysed and a third comparison is composed. Out of the case where the number of injector nozzle orifices were changed the case with 9 holes (case 7) comes out as most promising. For the second comparison the case with adapted concentrations to achieve the same lambda has the best properties. The third comparison exist out of a combination between the two previous results eventually ending in the most ideal case. The third comparison is done with a new composed case that has changed species concentrations of the trapped gas and 9 injector orifices (case 10). Out of this comparison this case comes out best with the best combustion efficiency and least emissions.

Palabras clave: Combustibles sostenible; e-fuels; proceso de combustión; reducción de emisiones contaminantes; CFD

Resumen

En los tiempos que corren, es importante dejar de depender de los combustibles fósiles. Cada vez se buscan más energías renovables alternativas. Esta tendencia también se ha dado en la industria automovilística, cada vez más gente busca un método de transporte respetuoso con el medio ambiente. Por ello, este estudio hace muy interesante que en el futuro se abandone por completo el uso de motores de combustión contaminantes con gasóleo. El combustible renovable considerado es el Oximetiléter (OME3). En este trabajo se evalúan las diferentes propiedades entre este e-combustible y el gasóleo utilizando el concepto de combustión oxicombustible para evitar la formación de NOx en los gases de escape. Las propiedades se analizan integrando tres comparaciones diferentes, una comparación en la que se cambia el número de orificios de la boquilla del inyector manteniendo las condiciones isoenergéticas, una comparación en condiciones iso-lambda e isoenergéticas. A partir de estas dos comparaciones se analizan los resultados y se compone una tercera comparación. De los casos en los que se ha modificado el número de orificios de la tobera del inyector, el caso con 9 orificios (caso 7) es el más prometedor. En la segunda comparación, el caso con concentraciones adaptadas para lograr el mismo lambda presenta las mejores propiedades. La tercera comparación se basa en una combinación de los dos resultados anteriores y termina con el caso más idóneo. La tercera comparación se realiza con un nuevo caso compuesto que ha cambiado las concentraciones de las especies del gas atrapado y 9 orificios del inyector (caso 10). De esta comparación, este caso resulta ser el mejor, con el mejor rendimiento de combustión y las menores emisiones.

List of figures

List of tables

Abbreviations

RoHR	Rate of Heat Release
CumRoHR	Cumulative Rate of Heat Release
IVC	Intake Valve Closed
CAD	Crank Angle Degrees
PMI	Indicated Mean Pressure
ISFC	Indicated Specific Fuel Consumption
TDC	Top Dead Centre
BDC	Bottom Dead Centre
CR	Compression Ratio
LHV	Low Heating Value
EOI	End of Injection
ID	Ignition Delay
EVO	Exhaust Valve Opening
SOC	Start of Combustion

List of symbols

Stroke	S
Bore	B
Displacement volume	V_d
Clearance volume	V_c
Compression ratio	$\boldsymbol{\varepsilon}$
Thermal efficiency	$\boldsymbol{\eta_t}$
Heat capacity ratio	$\boldsymbol{\gamma}$
Cumulative Rate of Heat Release	$\boldsymbol{Qac}$
Pressure	P
Volume	V
Temperature	T

Mixture fraction	Z
Equivalence ratio	Φ
Heat capacity at constant pressure	C_p
Heat capacity at constant volume	C_V

Index

REPORT

1 INTRODUCTION

1.1 Context and motivation

In today's day and age, it is important to discontinue our reliance on fossil fuels. More and more there is being searched for alternative renewable energy. This trend has also been taking place in the vehicle industry, more and more people are looking for an environmentally friendly transport method. As a result, this study makes it very interesting for the future to completely move away from polluting combustion engines on diesel. The renewable fuel under consideration is Oxymethylether (OME_3), what exactly this fuel entails will be discussed later in the manuscript. Switching to a completely new fuel naturally presents its challenges and necessary research. That is why this work investigates the impact of switching to this renewable fuel on the combustion process. Based on this analysis, we examine various parameters and adjustments will be made to optimize the combustion process and minimize pollutants. Thus, finally resulting in the most favourable case.

1.2 Objectives of the project

The objective of this work is to analyse the combustion performance of a compression ignition system fueled with Oxymetylether 3 (OME_3). So, the combustion efficiency can be improved while minimizing the emissions to the environment. This overall objective can be divided in the following partial objectives:

- First, some simulations were obtained using the OpenFOAM software. Here five different cases were achieved using OME_3 and one case where diesel is used as a reference, with the same compression ratio. In the first three cases using OME_3 a comparison where the number of injector holes will vary has been made to see the influence of this. The two other cases using OME_3-fuel we made an ISO-Lambda comparison by adjusting the concentrations (or adjusting the temperature).
- Second, a post-processing has been done using MATLAB code to achieve different graphs of the variables representative of the combustion process. From these graphs we could look at what crank angles it was interesting to have a comparison between the cases.
- Third, an examination was conducted looking at the different variables in the post-processing tool *paraView* and decided what variables are interesting to set out against each other. Most of these variables we set out in 2d and 3d plot to get the best idea of the situation.
- Fourth, conclusions were made depending on the achieved results and a theoretical research.
- Fifth, an optimum case was proposed based on the analysis.

1.3 Thesis outline

To achieve a comprehensive presentation and a systematic approach on the final conclusion, the report was structured into several distinct points:

- Introduction
- Theoretical background
- Methodology
- Results and discussion
- Conclusion

After the report a budgeting part was composed to achieve an insight into the cost of this project.

2 THEORETICAL BACKGROUND

2.1 Computational tools

2.1.1 OpenFOAM

OpenFOAM is the free software we used to create the different simulations of the cases. OpenFOAM stands for Open source Field Operation And Manipulation, it is an open source software used to process Computational fluid dynamics (CFD) developed by OpenCFD Ltd since 2004 [1].It is particularly suitable for solving (differential-)equations in simulations of physical processes by using the programming language C++ . Also, the Lib-ICE library was used, which is a library for internal combustion engines developed by The Internal Combustion Engine Research Group (Politecnico di Milano). It is a well-known software in all kind of areas of engineering and science.

All the information is stored in a couple of folders:

- Constant-folder: In this folder the physical specifications of the case are described such as for example the injector properties which returns the values of the Start Of Injection (SOI), the diameter of the injector holes, the mass and so on. This folder also includes a "flameletRegion0" folder with a "polyMesh" folder inside which defines the mesh for the case.
- Output-folder: Here all the different results of the variables of the simulation are collected in different text-files.
- Processor-folders: This folder also has different time folders named after the crank angles the simulation was run at.
- Species-folder: This folder shows all the concentrations of species over time of the various analysed substances.
- System-folder: This folder contains the files that determine the configuration and execution of the procedure to solve the case. It contains multiple text-files, one for example with all the time-steps, numerical tolerances, etc for the simulation run.

After the simulation was run, the next step is the processing of the data. For this purpose, the "reconstructTopoMesh" command is executed, indicating the time range for the processing. This last command creates all the time folders starting from crank angle -112.65 until crank angle 100. After a .foam file is created it could be opened in *paraVIew* to do the postprocessing there.

2.1.2 ParaView

The postprocessing of the .foam files is done in the software *paraView*, this is an open source program for visualising and analysing scientific data. So, a better understanding can be achieved of the qualitative and quantitative data of the simulations of the combustion process. It helps us to see where the certain variables are concentrated and how to adapt to it in the future.[2], [3]

2.1.3 MATLAB

MATLAB was used to generate graphs of the different variables to see progression over time as the crank angle varies. Here given MATLAB-scripts were used where some minor adjustments had to be made to post-process the cases.

2.2 Internal combustion engine [ICE]

To reach the step-by-step explanation of this project, a brief explanation of the operation of an internal combustion engine is done first. In this way, it is possible to build on our knowledge and reach well-grounded conclusions. In this project I will limit my explanation to the diesel case that works on the principle of self-ignition and does not make use of a spark plug.

2.2.1 Basic principale

An internal combustion engine is an engine that converts the chemical energy stored in the fuel to useable mechanical energy by transferring heat. There are two main types of engines that work by different principles, the two-stroke and the four-stroke engine. The number of strokes refers to the amount of movements of the piston in the cylinder to complete a full engine cycle. The two-stroke engine will not be considered in this explanations since this work has been performed on a 4-stroke engine, this is the one that will be explained bellow:

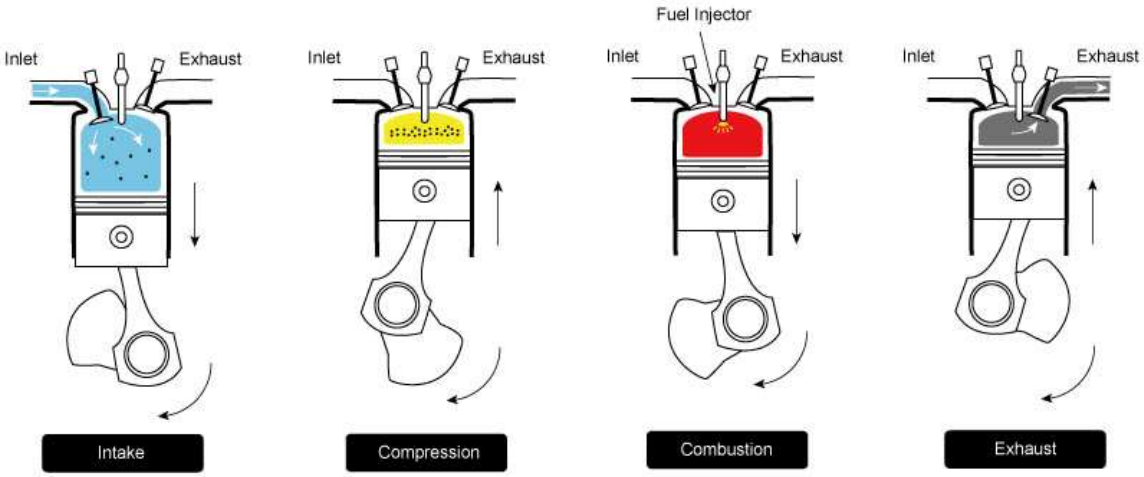

Figure 2.1: Different strokes of the combustion process [4]

This process to create mechanical energy follows a few steps who I will briefly explain:

1. **Intake:** During the intake stroke air is been drawn into the combustion chamber from the inlet by the opened valve while the piston is moving down. Unlike in traditional gasoline engines where a mixture of air and fuel is been drawn in.
2. **Compression:** In the compression stroke, the piston is moving up again while both the inlet and exhaust valves are closed compressing the air and heating it to a temperature higher than the ignition temperature of the fuel. Just before the piston reached its Top Dead Centre (TDC) where the combustion chamber has its smallest volume, fuel is injected into the cylinder

through the injector holes of the injector. This spray of fuel quickly ignites because of the high temperature of the air.

3. **Combustion:** This ignition of fuel creates pressure in the combustion chamber which lets the piston move downwards creating work and thus generating the desired mechanical power. The work created in this stroke exceeds the amount of work that has been put into the system to compress the air. During this stroke the gases decrease in temperature, pressure and density, opposite of the compression stroke. When the piston is approaching Bottom Dead Centre (BDC) the exhaust valve opens.
4. **Exhaust:** With the exhaust valve being open the piston moves up again pushing the exhaust gases out. An amount of exhaust gases will not leave the cylinder since it doesn't full close off the combustion chamber. When the cylinder is at its highest point again the exhaust valve will close again and this four-stroke cycle will repeat itself. So, the crankshaft will make two revolutions to complete the four-stroke cycle.[5]

2.2.2 Geometrical parameters of an internal combustion engine

In this part the basic geometrical parameters of an internal combustion diesel engine are expressed, these parameters are important to represent the performance of the engine. Later more information will be given about the specific values for the internal combustion engine used. The IV and EV both want to indicate respectively the Intake Valve and the Exhaust Valve. TDC also called Top Dead Centre is when the cylinder is at its highest position and when a crank angle of 0° is reached. When the cylinder is at its lowest position 180° crank angles later we talk about BDC. The width of the cylinder is given by the value B, the cylinder bore in mm. The total distance the cylinder can travel over is called the piston stroke S. The symbols V_d and V_c, which stand for the displacement volume and clearance volume, respectively, are still there. The clearance volume is the volume that remains in the cylinder when the piston is at its top dead centre.

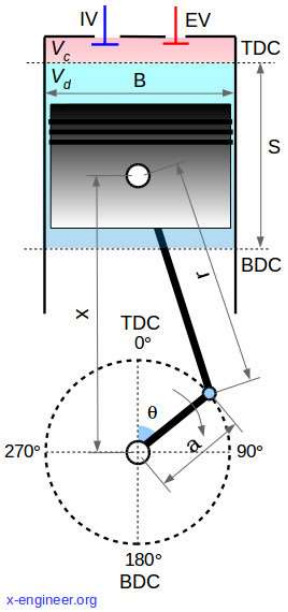

Figure 2.2 Geometrical parameters of a basic piston and cylinder [6]

The volumetric capacity (displacement) can now be given by following formula: [6]

$$\boldsymbol{Vd = S\frac{\pi B^2}{4}} \quad (1)$$

2.2.3 Influence of the compression ratio

The compression ratio is the value that is given by dividing the total volume of the cylinder when it's at its BDC divided by its clearance volume Vc, so this is a fixed value that depends on the geometry of the engine which can be calculated with equation 2.

$$\boldsymbol{CR = \varepsilon = \frac{Vmax}{Vmin} = \frac{Vc+Vd}{Vc}} \quad (2)$$

Later in the cases in our research there is being worked with a CR of 20, meaning that the total volume is twenty times greater than the clearance volume. Usually diesel-engines have a CR ranging from 12 until 24. A higher CR means that from a given mass of air and fuel mixture a higher amount of thermal efficiency can be retrieved which means that more mechanical power can be extracted, so the CR impacts the performance of an internal combustion engine. In the equation down below the relationship is shown between the thermal efficiency and the compression ratio.

$$\boldsymbol{\eta_t = (1 - \frac{1}{\varepsilon^{\gamma-1}})} \quad (3)$$

Also, the temperature of the air compressed in the cylinder is determined by the compression ratio because there is more heat extracted per amount of fuel. The higher compression temperature achieved would result in a shorter ignition delay and thereby reduces certain emissions such as carbon monoxide and hydrocarbon emissions. Another advantage of the shorter ignition delay is that less noise is emitted from the combustion process. On the other hand, a shorter ignition delay enables a better premixing which minimizes soot production. A higher CR also means that a higher in-cylinder combustion pressure would be reached. All of this, would mean that a higher compression ratio results in a more complete combustion, a better mixing of the fuel and thus ending up with a motor with better fuel economy. However, a higher compression ratio does also pose some disadvantages, these are some basic drawbacks:

- The higher pressure and temperature reached at higher compression ratios can cause an increase in in NO_X-emissions by thermal formation.
- Higher pressures are reached for the same amount of heat released which will result in more wear on the engine.
- The losses in terms of heat will become higher at the piston and head surfaces.

[6]–[8]

2.3 Thermodynamic variables

- **Rate of Heat Release**

The Rate of Heat Release (RoHR) also commonly called HRR is a variable that gives the amount of heat released from a fuel when it is combusted expressed in watts (W/time). It is a crucial parameter for optimising the combustion process and thus maximising the combustion efficiency and minimizing emissions. The correct adjustment of this parameter will thereby influence the fuel consumption and the reduce combustion noise. The classification of the phases of combustion is done by the rate of heat release.

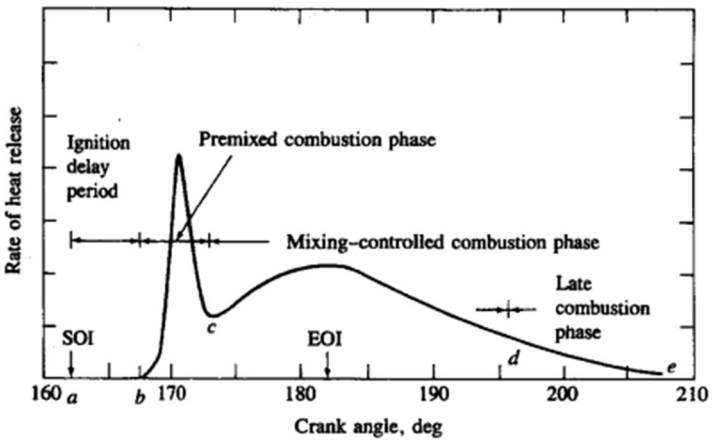

Figure 2.3 The different combustion phases shown with the rate of heat release [9]

The combustion process can be divided into four phases, namely ignition delay period, premixed combustion phase, mixing-controlled combustion phase and late combustion phase. The black line in Figure **2.3** shows the course of the graph for the rate of heat here the points start of injection (SOI) and end of injection (EOI) can be clearly seen.

Ignition delay period (a-b period): This phase starts at SOI of the fuel and lasts until the SOC. When the fuel enters the combustion chamber during this stage it has the form of a jet. This fuel than is surrounded by the compressed air and receives heat from it and vaporises. Thereafter, there is formation of the pre-flame reaction of the mixture, this is the period before the autoignition of the fuel where the vaporised fuel is mixing with the compressed air. Here the pressure in the cylinder starts to build up while there is no real rise in rate of heat release. There is a certain time between the SOI and the SOC, this time called the delay period can be divided into the chemical and the physical delay. The time it takes for the fuel to reach its autoignition temperature from the SOI is the physical delay. After this delay there is the chemical delay where the pre-flame reaction takes place it is the time from the ignition of the fuel and the appearance of the combustion flame. This

Premixed combustion phase (b-c period): Once the fuel undergoes autoignition due to the high pressure and temperature in the combustion chamber, a rapid release of energy happens because of the fuel getting burned, this can be clearly seen by the slope of the graph of rate of heat release. The mixture in the combustion chamber during this phase is heterogeneous which results in appearance of flames where high concentrations of mixture can be found, the

heat created from this than starts the burning of the surrounding lower concentrations. During this period there is no control over the amount of that is burned. This phase lasts until the point c where a local minimum is achieved.

Mixing-controlled combustion phase (c-d period): In previous phase all the fuel that was gathered during the ignition delay phase was burned. However, the injection of the fuel hasn't ended yet and the newly injected fuel while burn nearly immediately because of the high temperature mixture available and the excess amount of oxygen available in the combustion chamber. Because of this, the rate of fuel injection can be regulated to manage the rise in cylinder pressure. During this phase again, a rise in rate of heat release can be seen around the end of injection where after it decreases again.

Late combustion phase (d-e period): During this phase the expansion stroke is already happening, the maximum pressure has already been reached and the combustion is over, but heat is still being released and during this phase fuel is still being burned. [9], [10]

- **Cumulative Rate of Heat Release**

This parameter is also an important one to characterize the combustion efficiency of an internal combustion engine, it represents the integral of the RoHR and thus the area under curve and is a property to represent the total efficiency and not the current value at each timestamp. The cumRoHR (Qac) can be given by the equation (4): [11]

$$\boldsymbol{Qac} = \int \boldsymbol{dQ} = \int \frac{\boldsymbol{\gamma}}{\boldsymbol{\gamma - 1}} (\boldsymbol{PdV} + \boldsymbol{VdP}) \quad (4)$$

- **Combustion efficiency**

The ratio between the total amount of energy in the fuel and the amount of energy used to carry out useful work is known as the engine efficiency of an internal combustion engine. Combustion efficiency in general rises with an excess amount of oxygen being present this does result in a higher level of emissions such as an increase in in CO_2 and H_2O-levels.

- **In-cylinder pressure**

This is the pressure inside the combustion chamber of the cylinder, this value varies during the 4 strokes and gives us more information of the progress of the combustion. During the intake stroke for example, a low pressure is achieved by the downward movement of the piston, drawing air into the cylinder. In the oncoming crank angles, the pressure rises until a peak is reached where after the pressure drops again.[9]

- **Mean Indicated pressure (PMI)**

  Moreover, often called MIP, is the average of the pressure in the indicator diagram. An example of an indicator diagram of a four-stroke engine can be found in Figure **2.4**. In this diagram, the connection between the pressure and volume during one work cycle is shown. Pi refers here to the indicated pressure, while Pe and Pz are the effective pressure and loss pressure respectively. The area between the lines e and k shows the positive work that is delivered during the expansion stroke. The area between the lines v and s shows the negative work that has to been done to exchange the in-cylinder charge, the resulting work will be the sum of the positive and negative work.[11]

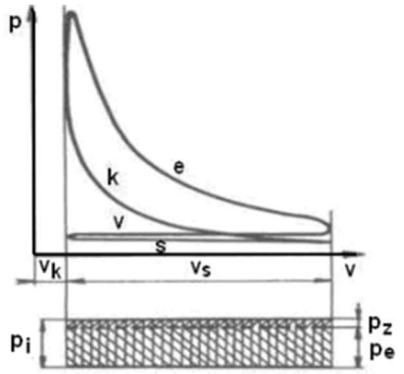

Figure 2.4 Indicator diagram of a four-stroke engine [11]

- **In-cylinder temperature**

  The in-cylinder is a very important parameter to keep track off because it heavily influences the mass and viscosity of the gasses in the cylinder which influences the peak pressure. Also, this value impacts the heat transfer to the cylinder walls. [12]

- **Mixture fraction (Z)**

  This parameter gives the mass fraction of a mixture of one substance to another substance in non-premixed combustion, in this case the substances being fuel and air. Later on, besides the mixture fraction Z also the equivalence ratio Φ will be discussed. The equivalence ratio gives us the ratio of fuel to air-mass to that of the stochiometric ratio and it is a very important parameter for IC engines because it gives us more information of the pollutants produced and how to deal with them by doing some tuning. Mixture fraction can be interpreted as a normalised fuel-air equivalence ratio. Also, the equivalence ratio gives us more information of the released energy and if the mixture can be even combusted this again gives us the information to do some performance-tuning. [13], [14]

- **Indicated Specific Fuel Consumption (ISFC)**

  An internal combustion engine's efficiency at converting fuel energy into productive work can be given by the indicated specific fuel consumption ISFC, typically indicated by the amount of fuel consumed in grams per kWh. ISFC is dependent on a number of factors such as design,

which fuel is being used and what engine conditions is operated on. For this reason, this parameter can be affected by a number of factors.[15]

- **Gamma-value**

  The gamma-value also known as the heat capacity ratio, gives the value of the heat capacity at constant pressure divided by the heat capacity at constant volume. [16]

$$\gamma = \frac{C_p}{C_V} \tag{5}$$

2.3.1 The injector

Fuel injection is one of the most crucial components of a diesel engine and has to be controlled very precisely. The timing of the injection has to be at the right crank angle since the whole combustion is based on this. In a diesel-engine the fuel and air are not premixed and thus when the fuel is injected the mixture in the combustion chamber is heterogeneous. However, it is utmost important that the fuel is mixed thoroughly with the air and the fuel is vaporized rapidly to ensure a complete combustion. Because of all these reasons the injector and its nozzle should be well designed, that's why the number of injector holes is one of the parameters that later will be changed to compare the different cases.[17]–[19]

- **Injection Pressure**

  The pressure of the injected spray is very important for the combustion efficiency and thus important for the performance of the engine, it also highly influences the emissions. In diesel engines using a common rail injector, a pressure of 1500 to 2000 bar can be expected. Increasing the injection pressure leads to better atomisation improving the vaporising and the mixing. For the usage of OME-fuel a higher injection pressure might be needed to compensate for the less energy because of the lower LHV.[20]

- **Swirl**

  The configuration of the injector, the combustion chamber geometry and the swirl are all adjusted to each other so if later there will be talked about the cases where the amount of injector holes are changed, this might be an important subject to discuss. Swirl is the rotational motion the air makes when entering the combustion chamber, and it increases the mixing of fuel and air so a more homogeneous mixture can be achieved, which again result in less emissions and a better fuel economy and combustion efficiency. [8], [21]

2.4 Influence of the composition of the gas in the cylinder: Oxy-fuel combustion

In the cases later discussed Oxy-fuel combustion is used, this means that the fuel is burned using pure oxygen or a mixture of pure oxygen with combustion gas instead of using atmospheric air. This means no insertion of nitrogen in the system which leads to a combustion that does not emit NOx as pollutant. Another advantage is that only the oxygen has to be heated instead of all the substances in the air leading to a better fuel economy. In our tests an oxy-fuel combustion was used where with recirculation of the combustion gasses (CO_2 and O_2), if only pure oxygen was being used a too high of a flame temperature would be reached. The resulting CO_2 can also be stored and used for other purposes. [22], [23]

2.5 H_2O-recirculation

One of the measures to improve the combustion efficiency by increasing the specific heat capacity ratio is the use of H_2O-recirculation. H_2O-recirculation works by recirculating water vapour and other exhaust gasses back into the intake resulting in better emissions. The exhaust gasses which are recirculated absorb heat, resulting in an increase in specific heat capacity. The lower heat capacity than results in a lower combustion temperature which in the case of no oxy-fuel combustion would result in lower NOx formation. [24]

2.6 Influence of the fuels

One of the big reasons that there are less and less cars on the road that run on diesel are its emissions that are released into the air. Diesel engines expel high levels of NOx and soot, that is why there is being searched at other types of fuel. In this part of the report, an analysis of the different properties of OME_3 and diesel will be made where conclusions on their impact on the combustion process will be drawn from. At a complete combustion of diesel the chemical equation would be: [25]

$$C12H28 + 19\,O2 = 12\,CO2 + 14\,H2O$$

Since in reality a complete combustion won't happen, the equation would look different with other by-products.

The alternative fuel used is oxymethylene ether-3 (OME_3) it is a synthetic oxygenate fuel, the chemical composition can be seen down below. What is remarkable on the chemical composition of oxygenate fuels is that oxygen atoms are bound between the carbon atoms. There are more types OME-fuels, the difference between them is just the amount of oxymethylene "$(CH2O)$" groups in the chain, in our case there are three. The number of groups largely determines the physical properties. OME-fuels are obvious fuels to investigate for internal combustion engines as the physical and chemical properties are very similar to those of diesel, allowing conventional diesel combustion systems to be used without significant modifications. Another great advantage of this fuel is the possibility of environmentally friendly production, it is produced via the methanol route. And could in that way also be produced again from the CO_2 combusted during its usage. [26]–[28]

CH3O(CH2O)3CH3

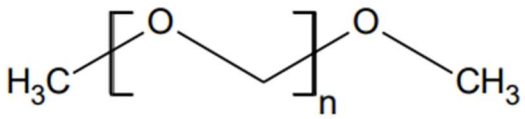

Figure 2.5: Structure of OME-fuel[29]

With an oxygenated fuel is meant that the fuel consists of ingredients or additives to enhance the level of oxygen. With OME_3 oxygen can clearly be seen in the structure what is not in the case of diesel, this higher level of oxygen makes sure that the combustion is more complete and less by-products such as carbon monoxide are formed. However oxygenated and unoxygenated fuels differ in a number of other properties besides just the oxygen-content.[30]–[32]

Table 1 Fuel properties.

	Diesel conditions	**OME_3 Conditions**
Density[kg/m³] @T=15°C	839.91	1046.55
Viscosity [Pa*S] @T=15°C	0.0016	0.0021
Cetane number [-]	54.18	78
LHV [MJ/kg]	44.5	19.6
Initial Boiling Point [°C]	155.1	155.04
Final Boiling Point [°C]	363.1	201.1
Oxygen content [% m/m]	0	47.5
Air fuel relation	15.09	8.07

The similar initial boiling point in Table **1** of both OME compared to diesel shows that it would suit as a valid alternative fuel. One of the properties of the fuels that introduces a difference in the combustion is the Low Heating Value (LHV), in the simulations this is assumed to be a constant. The LHV represents the amount of heat released when the fuel is fully combusted in normalized conditions of pressure and temperature. A lower value for OME_3 can be seen in Table **1** compared to diesel, this would suggest a lower efficiency for OME_3 but with the higher density this gets mostly compensated. Another important property of "diesel-like fuels" is the cetane number. The cetane number indicates at what speed the fuel can be combusted and what compression is needed for the ignition of the fuel. The higher the cetane number of the fuel, the shorter the ignition delay. In Table **1** a cetane number of 78 can be seen for OME_3 while diesel has a lower number of 54.18 which leads to a higher efficiency. [33], [34]

2.7 Lambda value

"Lambda represents the ratio of the amount of oxygen actually present in a combustion chamber compared to the amount that should have been present in order to obtain 'perfect' combustion."

This means that when the total amount of oxygen available in the combustion chamber corresponds to the amount of fuel, lambda will have a value of one. Lambda can be interpreted as the opposite of the air equivalence ratio that has been discussed earlier in section 2.3. If there would be too much oxygen available in the mixture in relation to the amount of fuel, there can be spoken of a lean mixture and the lambda value will be greater than 1. When the opposite occurs and more fuel is present in relation to the amount of fuel, the mixture is called rich and the lambda will be lower than 1. This lambda value will thus also be different when using different fuels, not an equal amount of oxygen is needed to burn diesel as for OME-fuel. For this reason, an Iso-lambda comparison will be done to have a better insight into the different combustion parameters, and to cope with the change of the fuels.[35]

2.8 Emission variables

Only certain variables were looked at and investigated better, in this part of the report I will give a better explanation why certain variables were taken into account and what their influence is on the combustion process. All these different variables have a certain connection with each other, one variable can influence the other either positively or negatively. For example, maximising the combustion efficiency is not necessarily accompanied by lower emissions.

- **Oxygen-content (O_2)**

Oxygen is the driver of the combustion and for this one of the most important parameters to take into account, without oxygen no heat would be created. Normally when no oxy-fuel combustion would be used, we would have to deal with normal air for the combustion consisting mainly of 21% oxygen, 78% nitrogen and 1% other gasses. But since pure oxygen is used, no energy is lost to the other gasses. Oxygen combined with the fuel forms CO_2 and H_2O as seen in the chemical equation in section 2.6. The importance is thus having enough oxygen available for creating the best efficiency and the least amount of emissions

- **CO-content**

As the combustion is never fully complete, byproducts such as carbon monoxide will be formed as well. These by-products are very undesirable because it is poisonous and very polluting to the environment, contributing to climate change. Often this is controlled by exhaust gas recirculation (EGR), which recirculates an amount of exhaust gasses back to the engine intake.[5], [36]

- **HC-content**

Because not all the fuel is consumed during the combustion process, the leftover fuel will undergo certain reactions such as the formation of hydrocarbons.[5]

- **Soot-content**

Soot is the black substance of particulate matter that is formed during the combustion process of hydrocarbons, it is more likely to be formed when there is an abundance of oxygen and at high combustion temperatures. This substance is rather undesirable and poses significant health issues. In the automotive industry particulate filters “DPF’s” were introduced to minimize emissions to the environment. Stricter laws and requirements are also being imposed on vehicles that they must comply with in order to enter certain zones or to be even allowed on the road at all. All of this makes soot-content an important variable to discuss for internal combustion engines. A good approach to solve this issue is using fuels that produce little to no soot-content, this is where OME_3 and OME in general comes in. As previously mentioned there are no carbon-carbon bounds in OME-fuel what makes this an almost soot-free fuel because there are no soot forming components. [26]

3 METHODOLOGY

3.1 Explanation of the different cases

3.1.1 The reference case

The reference case consists out of the original diesel case, the other cases are compared with, the case is also called case0 and water recirculation was used here together with oxy-fuel combustion. The engine was used on fully loaded conditions at an rpm of 3500 and a compression ratio of 20. The other boundary conditions can be found in Table **2**. These boundary conditions will also be the basis for compiling our other cases.

Table 2 Properties of the reference case.

	Initial reference (diesel) case with H2O recirculation
Number of Holes	7
Diameter [µm]	134
Amount of fuel [mg/cc]	62.3
Lambda	1.21
SOI [CAD]	-12.4
T(IVC)[K]	474.6
P(IVC)[Bar]	2.58
O_2-concentration(IVC)[-]	0.3103
H_2O-concentration (IVC) [-]	0.2602
CO_2-concentration (IVC) [-]	0.4294
Mass(IVC) [kg]	0.000856
EGR[%]	67
TLiner(IVC) [K]	382.3
TcylHead(IVC) [K]	500.5
TPiston(IVC) [K]	482.59

The first comparison are the cases from 5 until 7, in all of these three cases OME_3-fuel was used. In these cases, only the number of injector holes were varied whereby also the diameter of the holes. Also, a same lambda and Iso-energy conditions were used together with a compression ratio of twenty with H_2O recirculation and oxy-fuel combustion. With the iso-energy conditions is meant that the same amount of fuel is injected for all the three cases. As type of combustion oxy-fuel combustion was used with an optimised combustion chamber of the CMT-building. For the remainder of the boundary conditions the same values were used as for the reference case. In the Table **3** below a small overview

of these conditions can be found. The reference (diesel) case will also be included in the comparison to see what kind of improvements are achieved.

Table 3 Properties for the different cases of the number of holes comparison.

	Case 5	**Case 6**	**Case 7**
Number of Holes	7	8	9
Diameter [µm]	187.4	175	165
Amount of fuel [mg/cc]	136.7	136.7	136.7
Lambda	1.38	1.38	1.38
SOI [CAD]	-12.4	-12.4	-12.4
T(IVC)[K]	474.6	474.6	474.6
P(IVC)[Bar]	2.58	2.58	2.58
O_2-concentration (IVC)[-]	0.3103	0.3103	0.3103
H_2O-concentration (IVC) [-]	0.2602	0.2602	0.2602
CO_2-concentration (IVC) [-]	0.4294	0.4294	0.4294
Mass(IVC) [kg]	0.000856	0.000856	0.000856
SOI_P [Bar]	59.21	59.07	59.05
SOI_T [K]	904.23	903.85	903.36
SOC [CAD]	-9.02	-8.82	-8.81

The next comparison of the cases that will be done is the one seen in Table **4**. Here either the concentrations (case 8) or the temperature (case 9) was changed to get an Iso-lambda comparison with the diesel case (λ=1.21). A difference of the mass of gas can be seen in case 9 compared to all the other cases because of the higher temperature that was used at IVC. The higher temperature results in a lower density, also resulting in a lower mass. The other boundary conditions are the same as mentioned above for the cases of the number of holes comparison.

Table 4 Properties for the cases of the Iso-lambda comparison.

	Case 8	**Case 9**
Number of Holes	7	7
Diameter [µm]	187.4	187.4
Amount of fuel [mg/cc]	136.7	136.7
Lambda	1.21	1.21
SOI [CAD]	-12.4	-12.4
T(IVC)[K]	474.6	541.8
P(IVC)[Bar]	2.58	2.58
O_2 -concentration(IVC) [-]	0.273	0.3103
H_2O-concentration (IVC) [-]	0.2789	0.2602
CO_2-concentration (IVC) [-]	0.4481	0,4294
Mass(IVC) [kg]	0,000856	0,00075
SOI_P [Bar]	58.90	57.38
SOI_T [K]	899.42	1000.5
SOC [CAD]	-8.59	-9.23

3.2 Working procedure

Firstly, the simulated cases were simulated using OpenFOAM software. Then, the cases got proposed to me and they were divided into the two comparisons mentioned above. To make a first analysis, a MATLAB-script was made to so the course of the different variables and a decision was made over which variables will be discussed. Once the graphs were obtained, the decision was made at wat crank angles plots would be created to get the most information and where the biggest differences between the cases are. After that, the .FOAM files were created and the *paraView* contours were created and combined in inkscape. Now, the analysis of the results could start. For this, research was done of every parameter we were going to asses and what their correlation is with the combustion process. Also, the different properties of the fuel and their influence were assessed. With this knowledge a reasoning could be constructed for the differences in variables using sources although they were hard to find since this subject is not very heavily researched yet. The results of this reasoning will be discussed in section 4.1. Once every of this parameter was assessed for each comparison the best case was chosen. Out of these two best cases a final configuration was constructed from which a conclusion was drawn.

4 RESULTS AND DISCUSSION

4.1 Results

4.1.1 Number of injector holes comparison

- **Thermodynamically comparison**

The in-cylinder pressure graph seen in Figure 4.1 has the usual shape for an internal combustion engine. You see the difference between the slopes of the graph this is due to the delay between the start of injection and the start of combustion, the slope changes only at around -9 CAD while the SOI is at -12.4 degrees. Later a decrease in the graphs slope can be seen when the peak value of the pressure is approached at more or less 7.5 CAD. For the in-cylinder pressure a higher pressure can be seen for the case with the highest number of holes (nine holes) while the pressure seems to be more or less the same for the other two cases. Also, the In-cylinder temperature can be seen in Figure 4.1, here again a higher in-cylinder temperature is seen for the nine holes case in general while the other two cases have a similar temperature. Also, the difference in slopes of the graph can be seen more clearly than in the in-cylinder pressure graph. However, the peak of the temperature is not at the same amount of CAD as the pressure peak but it is later. The vertical lines in the in-cylinder temperature graph show the difference between the start of combustion between the cases and the differences between the "CA90's" of the cases. CA90 shows the crank angle at which 90% of the fuel is burnt. Although the SOC of the nine holes case has a SOC which is a tiny bit later than the other two cases, the fuel is burned faster seen that the CA90 is lower. When changing the number on injector holes, this influences a lot of parameters such as sector size, injector diameter, liquid length, penetration, and atomization. Each of these parameters than influences the in-cylinder temperature and pressure on their own way. [9]The injector diameter decreases when increasing the number of injector holes, this makes for smaller fuel droplets. These smaller fuel droplets tend to evaporate faster and ensure a better atomization. In addition, a smaller diameter hole can also lessen the spray penetration and the liquid length since it causes an earlier start of the second break-up regime. A higher penetration could lead to impingement of the fuel on the piston or the cylinder which leads to a worse combustion. All of these positive influences lead to a faster burning of the fuel and higher levels of in-cylinder pressure and temperature.[37], [38]

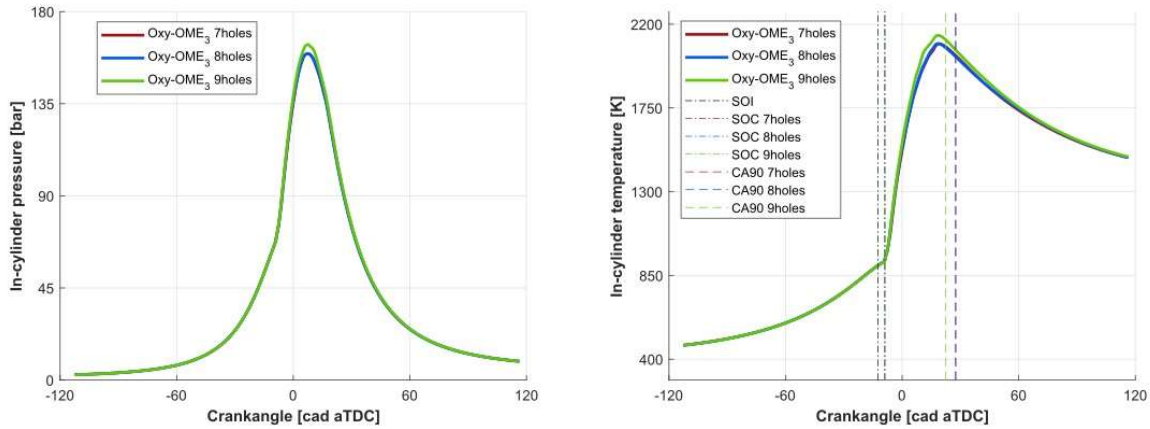

Figure 4.1 In-cylinder pressure and temperature comparison for the hole number study.

When looking at the temperature contours of the different cases in Figure 4.2, again there can be seen more high temperature fluid for the 9 holes cases compared to the other two cases. Crank angles were chosen in the period where the temperature is rising very fast, around the peak and when the temperature is dropping again. Especially just around the peak temperature which gets achieved close to 16.35 CAD, more yellow, meaning a higher temperature can be spotted. On the contours of 16.35 CAD and 10.35 CAD a higher temperature can be spotted at the end of the jet which is due to the better evaporation and atomisation. In the last two contours we still see less dark colours and more orange because of the higher temperature.

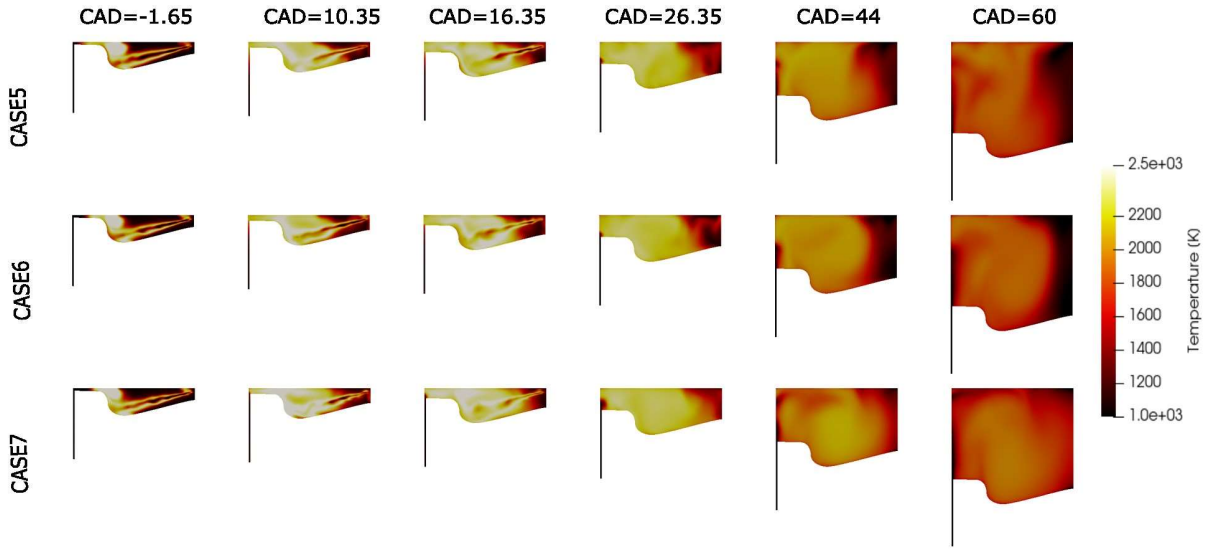

Figure 4.2 Temperature contours comparison for the hole number study.

Previously we already had a look at the Rate of Heat Release graph and the different combustion phases that can be recognised in it in section 2.3. After the first phase (ignition delay period) where no real rise in rate of heat release is formed, we enter the premixed combustion phase where the peak of the RoHR is formed. In Figure 4.3 the RoHR is shown for the hole number study. The slope is formed here very fast, in our case the slope and the peak of the 9 holes case is the highest. In this phase the high concentrations of mixture start to burn first, where after the lower concentrations start to burn because of this heat. Better evaporation and atomization will result in higher concentrations of mixture which will burn faster causing a more rapid release of heat, this phase lasts until a minimum is achieved

again. In the next phase of mixing controlled combustion all the newly injected fuel will burn because of the high temperature of the mixture and excess amount of oxygen, during this phase a 2nd maxima are achieved. Here, a higher energy and faster combustion is achieved in the 9 holes case, recognized by the graph being above the 7, and 8 holes cases in the beginning of this combustion phase where after dipping below again.

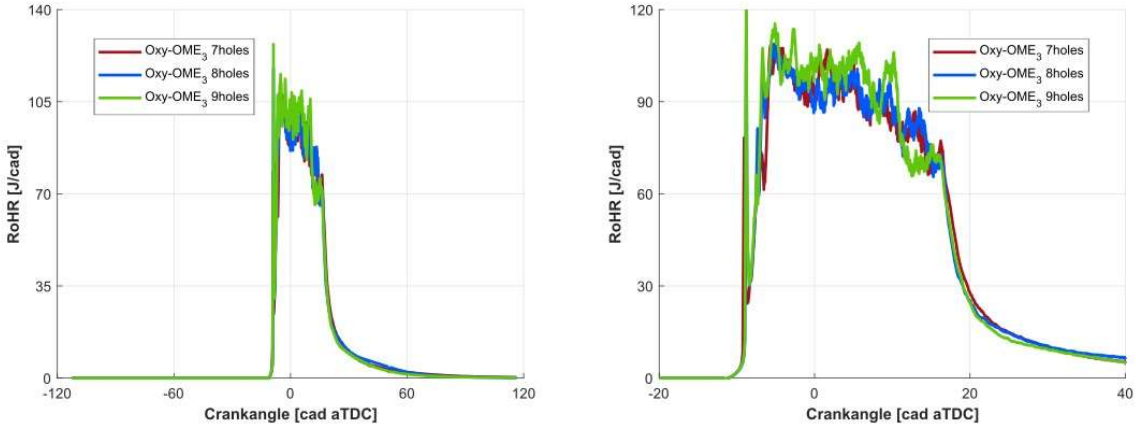

Figure 4.3 Rate of Heat Release comparison for the hole number study, with the right one being a zoom.

Figure 4.4 presents the results of the normalized cumulative heat release for all the cases. This parameter indicates how much of the available energy in the fuel was actually used and converted to work. For all the cases it is possible to see that almost all energy contained in the fuel was consumed once the end of the curve is close to 1 (or 100%). Furthermore, the case with 9 holes present a little higher of normalized cumRoHR, which means that this case shows a more completely combustion than the others. Moreover, this parameter also indicates the combustion efficiency since it is calculated considering the total energy and the energy consumed during the combustion processs in one cycle.

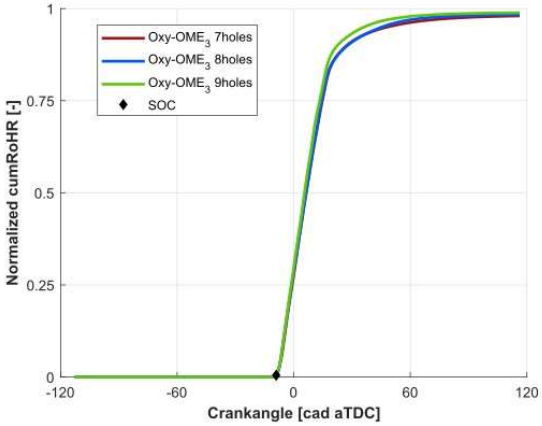

Figure 4.4 Cumulative Rate of Heat Release comparison for the hole number study.

In Figure 4.5, the heat capacity ratio *γ* for the different cases, this ratio is dependent on the composition and temperature during the engine cycle. A similar course can be seen over the crank angles for the different graphs, however the *γ*-value of the 9 holes case takes a bigger dip than the other cases. This is due to the temperature dependency of the capacity ratio, a higher temperature will result in a lower “gamma-value” and the 9 holes case has around the peak a significantly higher temperature as seen in Figure 4.1. The gamma-value can also be found in the RoHR-equation (2), the

different gamma value thereby also explains the differences in both the RoHR and CumRoHR of the 9 holes case and that of the other two cases. [39]

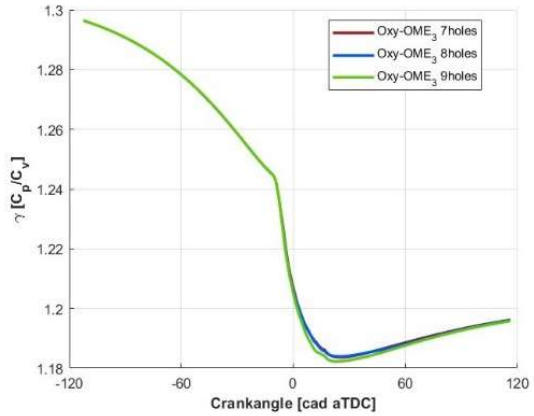

Figure 4.5 Gamma comparison for the hole number study.

- **Emissions comparison**

There can also be said a lot about the different working fluids in the combustion chamber. As previously mentioned Oxy-fuel combustion concept is used, this way no NOx has to be taken into account because there is no nitrogen present in the intake mixture, consequently there are no NOx emissions. To evaluate the emissions of the cases, different crank angles were chosen where the differences between the cases was the biggest, this explains the vertical dashed lines in Figure 4.6. At these crank angles (10.35, 21.35, 32.35, 44 and 60) the *paraView* contours were also plotted in Figure 4.7. When a first look at the oxygen-content in Figure 4.6 is taken an overlapping of the graphs of the 7, and 8 holes cases is seen. While the O_2-content of the case with 9 holes is certainly lower from a crank angle of 10.35 CAD. The lower content in the case with 9 holes is due to the better spread of the fuel inside the combustion chamber resulting in the oxygen being better consumed during the combustion process.

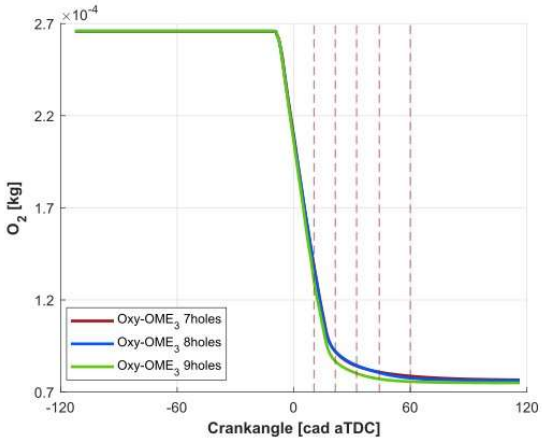

Figure 4.6 Oxygen-content comparison for the hole number study.

For most of the properties a 3D-plot was made with a certain threshold value so that only the contents above this value will be seen, in Figure 4.7 a threshold of 0.1 was used. The contours show that with the simulation evolution the oxygen presented inside the combustion is consumed progressively. In the first selected crank angle (10.35) there is a great amount of oxygen inside the combustion chamber,

even in the central region where the spray is developed. Moving to the other crank angles it is possible to see that the oxygen that was in the spray direction was consumed by the combustion process until the point just the oxygen in the crevice and near the centre of the geometry remains on the combustion chamber. Furthermore, it is noticed that using 9 holes (case 7), promotes a higher oxygen consumption due to the better atomization of the fuel. More injector holes lead to smaller injector diameter, which promotes smaller fuel droplets that better find the available oxygen resulting in a more complete oxygen consumption and combustion efficiency.

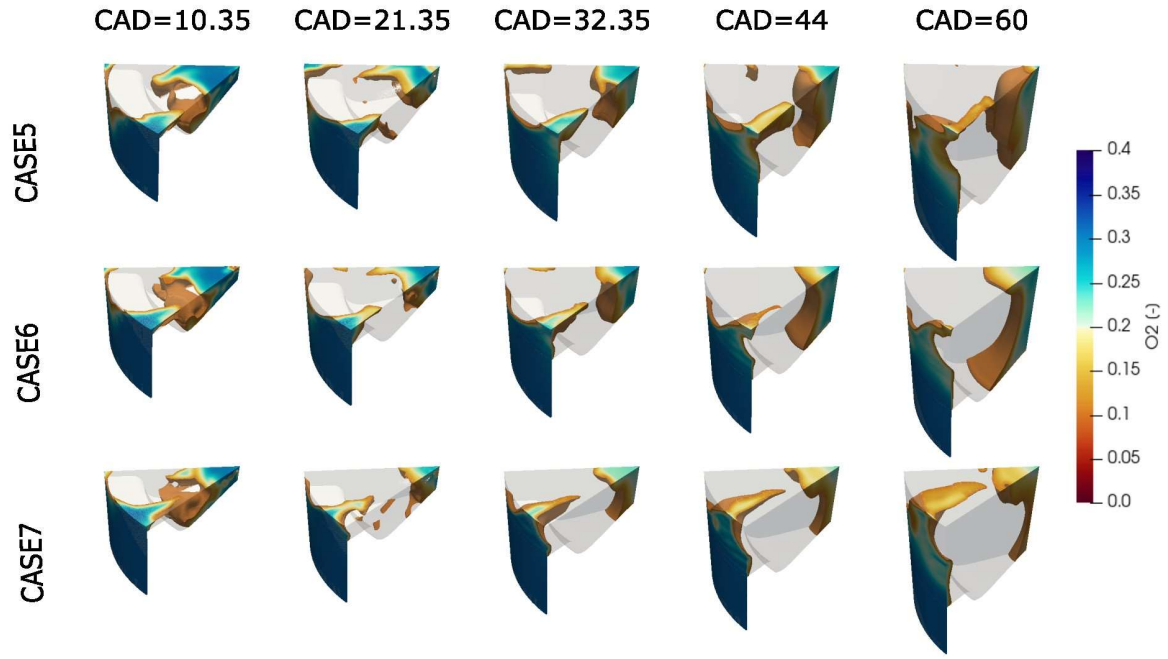

Figure 4.7 Oxygen-content 3D-contours comparison for the hole number study.

Figure 4.8 presents the C_2H_2 formation and consumption during the cycle for the simulations. This parameter is specially evaluated because it is the soot emissions precursor, and from its analysis it is possible to verify the OME_3 non-sooting nature. The magnitude of the acetylene for the diesel case is a lot more than that of the cases using OME_3-fuel (in the order of 10^{-6} to the order of 10^{-8}). This is due to OME_3 because there is no carbon to carbon bond in the fuel molecular structure, but having oxygen atoms between them as discussed in section 2.6. This way there is very little formation of the soot precursor C_2H_2, resulting in a negligible amount of soot.

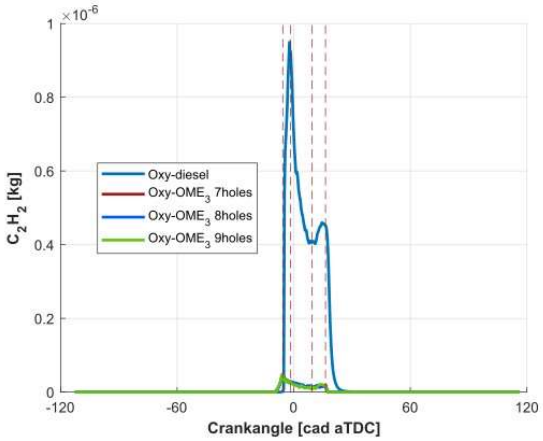

Figure 4.8 Acetylene-content comparison for the hole number study with the diesel case.

To see the influence of the amount of injector holes on the acetylene (C_2H_2) formation, a zoom was made and the diesel case was excluded seen in Figure 4.9. Crank angles were chosen over the whole course of the graph (-5.65, -1.65, 9.35 and 16.35) so a good comparison can be made. At first a peak of C_2H_2 formation is reached whereafter it declines again, at the peak nearly the same value was achieved for all three cases at a crank angle of -5.65 CAD. The 7 holes and 9 holes seem to be following the same course more or less while the case with 8 holes has a bit of a different trajectory with in general more acetylene formation. At the last crank angle, the biggest peak was reached for the case with the least amount of holes. In general these values are so small that it is hard to see the influence of the amount of injector holes on the acetylene formation.

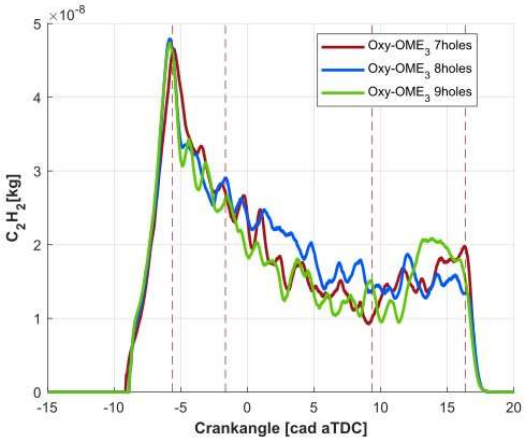

Figure 4.9 Acetylene-content comparison for the hole number study.

Figure 4.10 shows the 3D contours in *paraView* of C_2H_2 at the same crank angles of the vertical lines in Figure 4.9. Some different aspects can be highlighted at a crank angle of -5.65 the contours can be nearly assumed identical, at the following crank angles a decrease of the acetylene is expected if the number of injector holes is increased. As would be expected, a better fuel-air mixture and atomization which ensure a better combustion will reduce the emissions because less by-products are formed. [40]

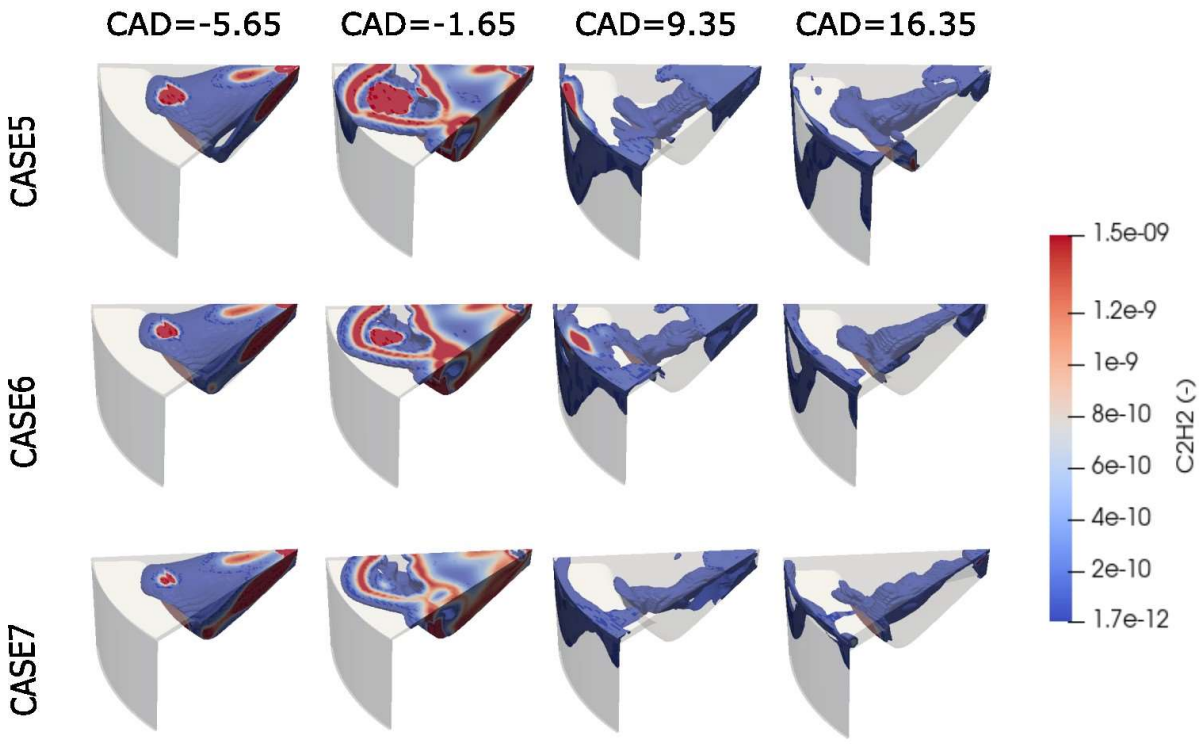

Figure 4.10 Acetylene-content 3D-contours comparison for the hole number study.

Figure 4.11 presents the H_2O cycle distribution for all the simulations. During the compression stroke and almost all the combustion processes, the water vapor distribution is very similar for the three cases. However, when the graph curves at a crank angle of about 16.5 CAD, it can be seen that the graph for the 9 injector holes is just above the other two and has the highest amount of water. This is due to a more complete combustion because of the better oxygen utilization so less byproducts are formed and more products are formed as would in the theoretical process such as (H_2O and CO_2) when the number of nozzle orifices is increased.

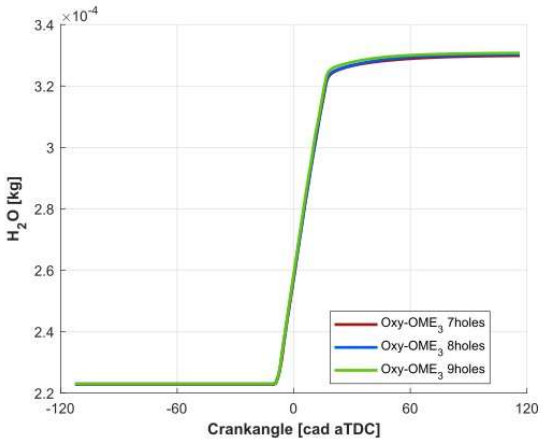

Figure 4.11 Water vapour-content comparison for the hole number study.

Figure 4.12, the 3D contours can be seen for water vapour content. Here the crank angles (10.35, 21.35, 32.35, 44 and 60) were used so we can see the H_2O-concentrations over a broad spectrum of

crank angles and after the curve that was discussed in the previous figure where the difference in water vapour content is more pronounced. A threshold of 0.31 was used to create the contours, so all the concentrations below this value won't be shown. At the first crank angle of 10.35 CAD, it is hard to decide whether the case with 9 holes has more water vapour concentration since at 10.35 CAD, there is less dark red. Hence, the H_2O is less concentrated, but the volume of H_2O that has a concentration higher than 0.31 is more significant. Looking further at higher crank angles, we keep seeing this trend, seeing that the volume of H_2O concentration spreads more to the middle of the piston. However, since the scale is over quite a small interval, we can conclude that from the crank angle of 21.35 (end of injection), the concentration is the highest for the case with nine holes with decreasing concentrations as the number of holes decreases.

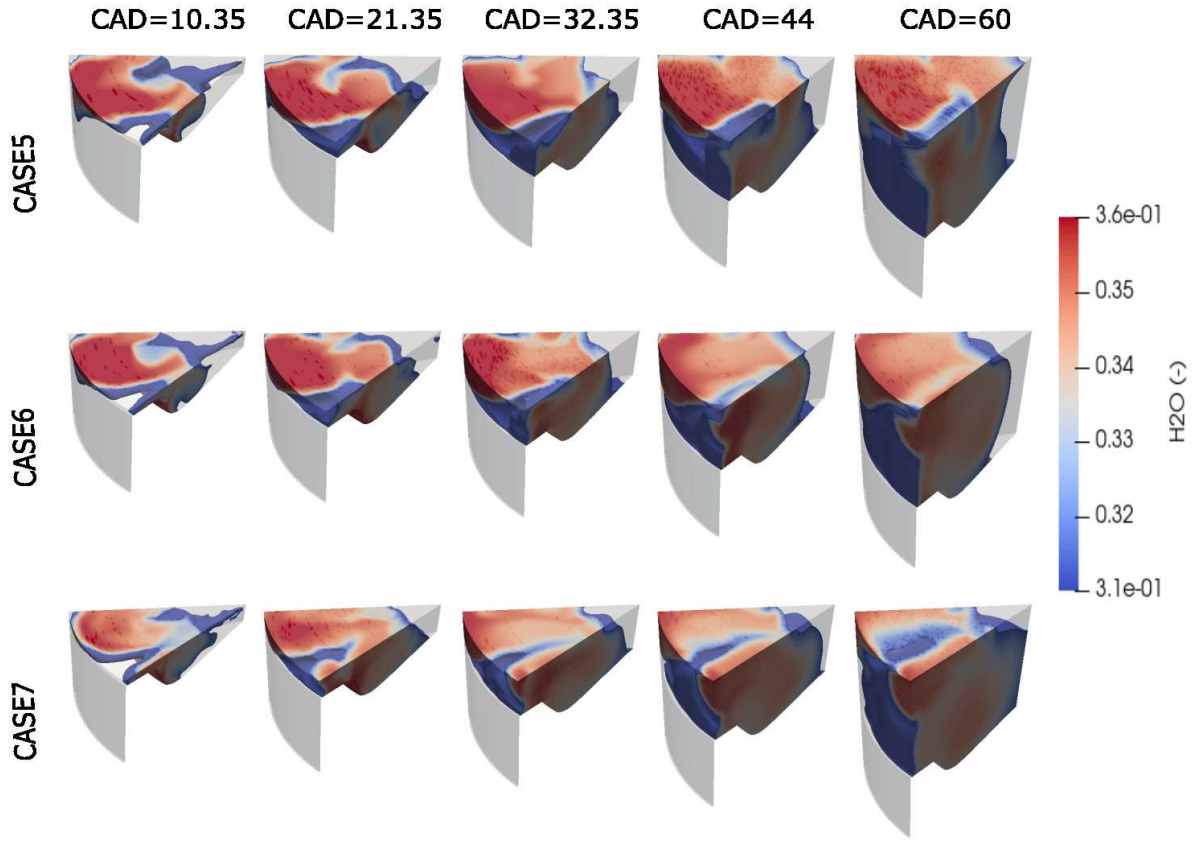

Figure 4.12 Water vapour-content 3D-contours for the hole number study.

In following Figure 4.13 the carbon dioxide graphs are discussed. The same crank angles were chosen for the water vapour-content because this is the spectrum where the biggest differences appear and they are shown by the red dashed lines in the figure. The three curves seem to mostly overlap until a crank angle of 10.35 CAD, there the levels of CO_2 concentration for the 9 holes case protrude above the other ones. At the following crank angles the CO_2 concentrations stick out more and more above the other ones while the 7 and 8 holes cases keep overlapping. From a crank angle of 60 CAD the blue graph for the 8 holes case starts to stick out above the case with least amount of holes as well, in the following crank angles the graphs come back together leaving a minor difference between them. Although the differences between the graphs look minor, still can be seen that the 9 holes case has the highest concentration, after that 8 holes case and the 7 holes case at last. The high levels of CO_2 are not wished because it is a greenhouse gas with bad influence on the environment. The environmental impact by CO_2 can be greatly reduced or even negligible since it could be captured and

reused for the production of OME-fuel. Although, a rise in CO_2-levels which is one of the main combustion products represents the completion of the combustion, since there is more fuel completely burned. Also, the because of the higher temperature reached in the case with 9 holes more CO_2 will be formed, since more fuel is being burned and more CO is further oxidised to CO_2.[23], [41], [42]

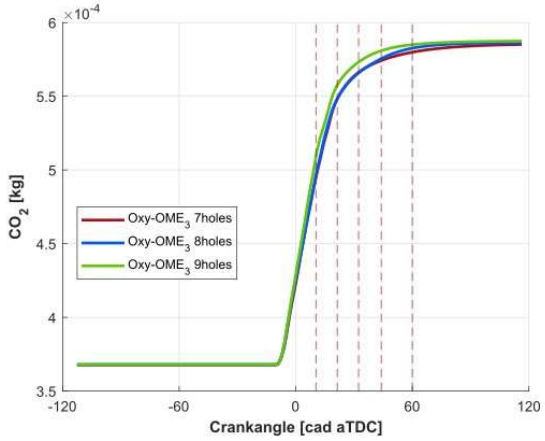

Figure 4.13 Carbon dioxide-content comparison for the hole number study.

In Figure 4.14 the 3D-contours are shown for the CO_2-content, on which the above findings can clearly be reflected. At crank angle 10.35 the 9 holes case clearly stands out with the highest CO_2 concentration. A threshold of 0.5 was used so lower concentrations will be see-through. The trend of higher CO_2 concentrations as the number of holes progresses is followed over all crank angles, where the 9 holes case the concentrations are clearly spreading until the middle of the cylinder.

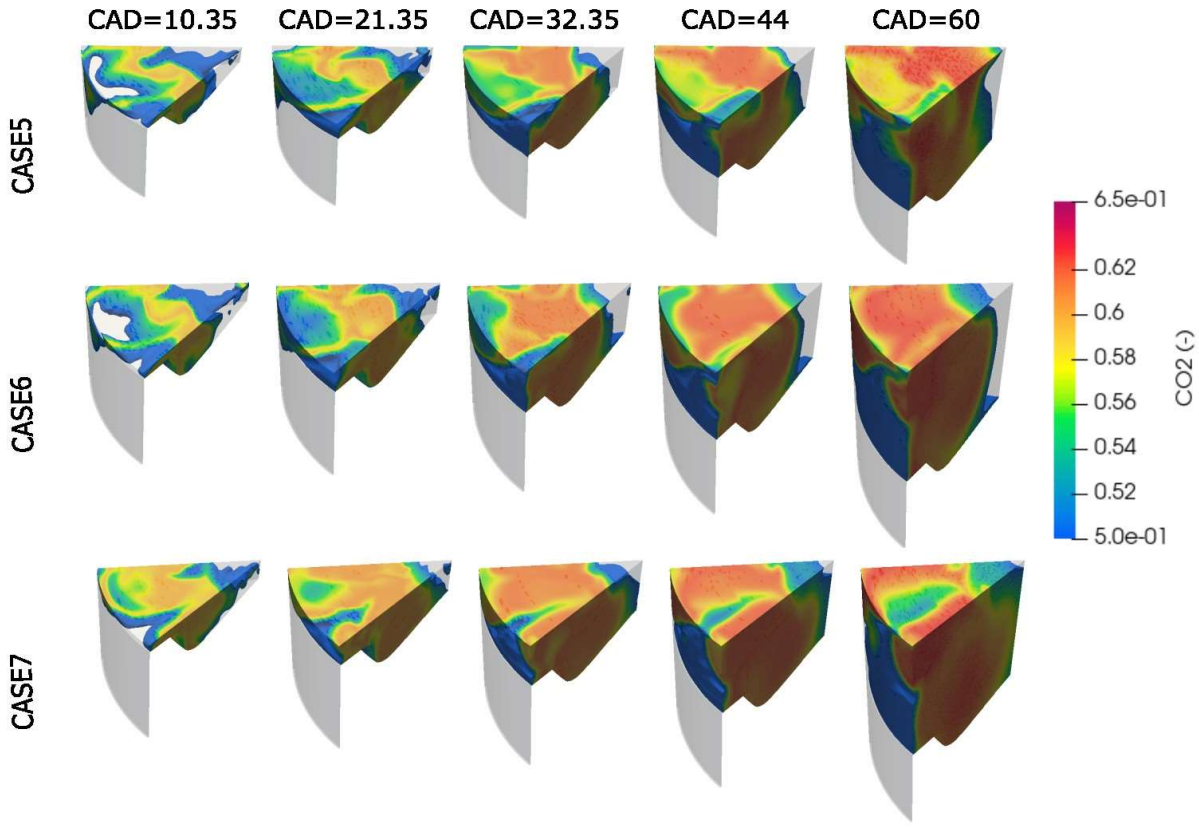

Figure 4.14 Carbon dioxide-content 3D-contours for the hole number study.

The hydroxyl-levels in Figure 4.15 are much higher for the oxygenated fuels compared to diesel, until the last crank angles are reached, there the diesel case surpasses and has the highest OH-levels. This rise in OH-levels starts during the fuel injection and continuing during the combustion process. This behaviour comes from the oxygen content on the fuel and, posteriorly more OH is formed during the combustion process leading to higher OH formation. However, as the combustion process is more complete, reaching higher in-cylinder temperature values, for the cases with OME3 the OH is consumed. The 7 and 8 hole cases both have a similar trajectory in terms of OH-levels while the 9 holes case clearly sticks out. However, in the end the OH-levels for the 9 holes case dip below the other two graphs again, this is due to the OH having reacted further to other byproducts. The more complete combustion process leads to more fuel being burned resulting in more OH coming free during the combustion, since this is a normal intermediate product during the reaction. Again, the same crank angles were used as for the CO_2 and H_2O contours. [28]

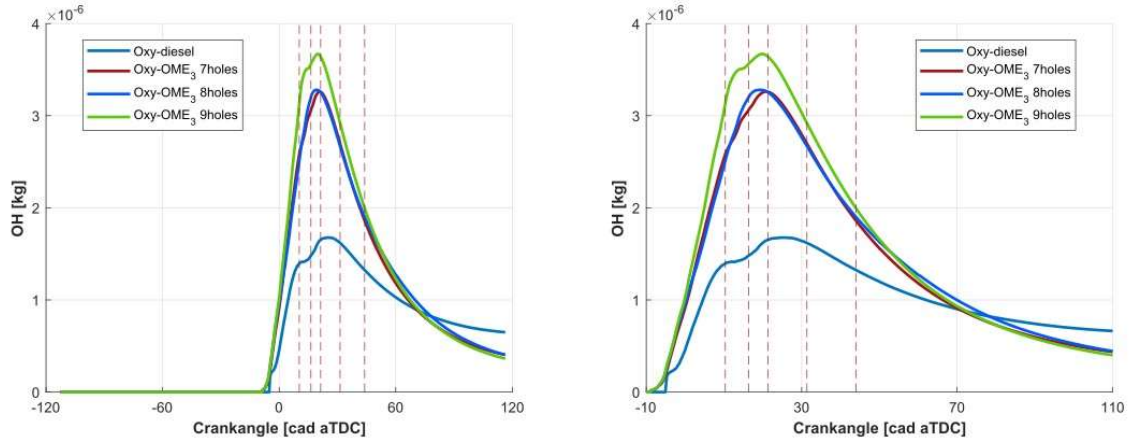

Figure 4.15 Hydroxyl-content comparison for the hole number study, with the right one being a zoom.

Following the contours in Figure 4.16, the same findings are seen as discussed above. A higher concentration for the 9 holes case over all crank angles while the diesel case has way less OH concentration. What we were not able to see on the figure above is that for the crank angles 10.35 and 21.35 CAD the case with 7 holes has a higher concentration than that of the 8 holes case.

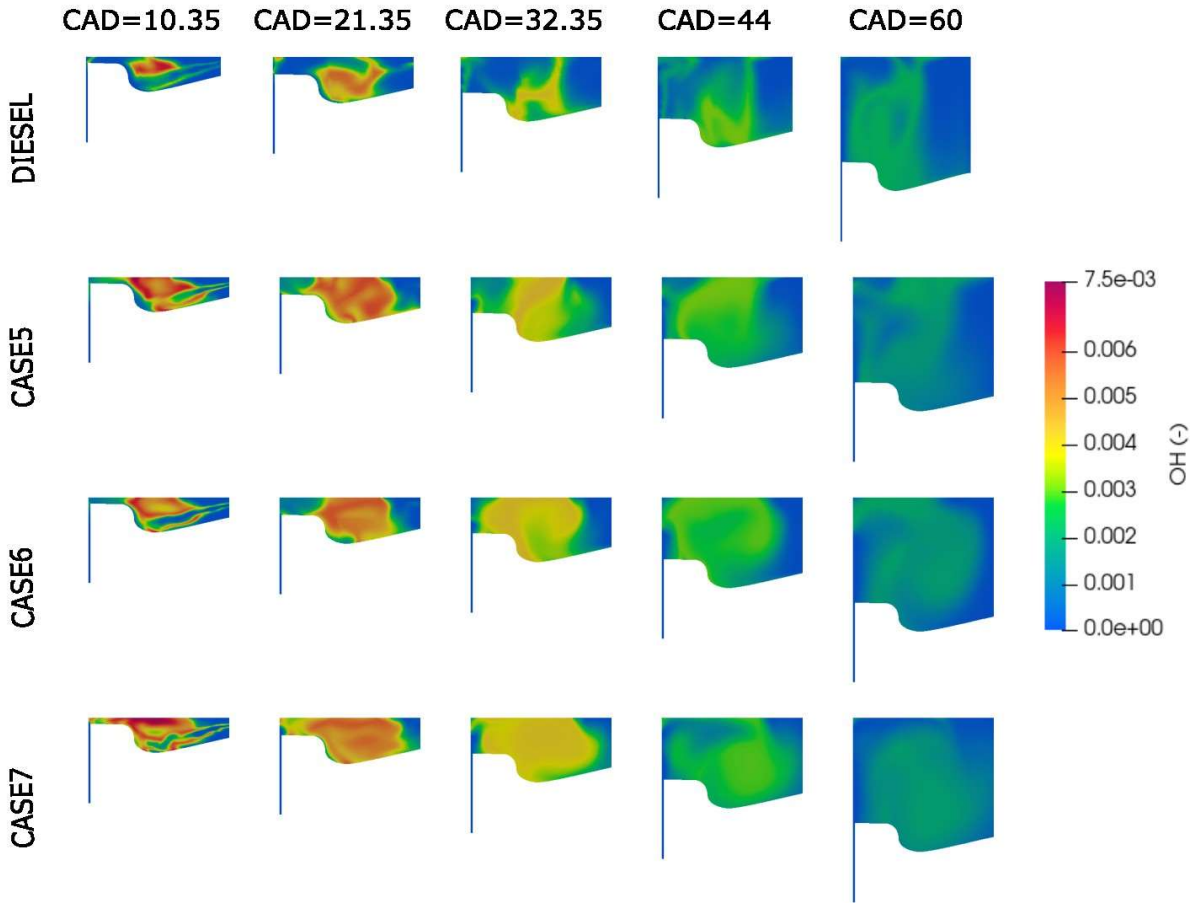

Figure 4.16 Hydroxyl-content contour for the hole number study.

- **Global engine analysis**

Figure 4.17 shows the total cylinder mass for all the three cases over three relevant equivalence ratios. One ratio represents the more stoichiometric condition (mt>1.05), another represent lean condition (mt>0.55) where there is a deficit of fuel and the last one represent rich condition (mt>1.75) where there is an abundance of fuel. It is possible to see that all cases show similar behaviour in the lean and rich conditions. However, in stoichiometric condition it is possible to see that the case with 9 holes present a better mixing rate, which is reflected in the better consuming of the mass in this condition. The case with 8 holes present an intermediate behaviour, consuming all the stoichiometric mixture around the CAD 60 while the case with 7 holes was not able to consume all the mass in this condition.

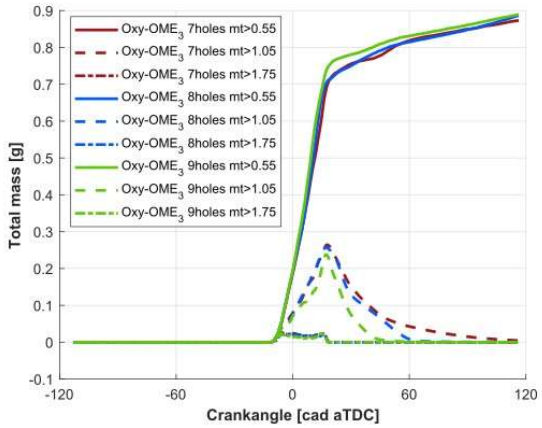

Figure 4.17 Total cylinder mass distribution comparison for the hole number study.

For the mixture fracture contours in Figure 4.18, again the crank angles (-1.65, 10.35, 16.35, 26.35, 44 and 60 CAD) were used so we can have a broad view of the mixture fraction along all crank angles. As previously mentioned smaller nozzle orifice diameters tend provide smaller fuel droplets. In the contours, a lower amount of fuel is seen for the 9 holes case as being progressed to the crank angles 10.35 and 16.35 since less red is seen this is due to the fuel being already burned. This is also due to that the fuel rich core of the jet of the injected fuel is smaller, because the fuel gets dispersed into more fuel streams but the total amount of fuel is the same for every case. In general, the smaller orifice diameter leads to better fuel-air mixing but this will be offset a little by the reduced turbulent energy by the jet. If than a look is taken upon the last two crank angles we can recognize that a lot of more blue is perceived in the cases with 7 (case 5) and 8 (case 6) holes, meaning that there is little to no fuel left in the middle of the cylinder. Which shows more fuel being left in contrary to our previous believes. But, we cannot conclude anything if this due to worse mixing since we don't know if the combustion is still consuming fuel. Afterall, there can be seen that the combustion efficiency will be better for the 9 holes case, so in the end most fuel will be burned here. If than a look is taken upon the contour at crank angle 26.35, a higher mixture fraction is seen in the 7 and 8 holes cases because of the amount of yellow still available. This yellow is at the outside of the cylinder so it will describe a bigger sector than the little bit more amount of mixture fracture (blue) is seen at the right, so in the middle of the cylinder for the 9 holes case. [18]

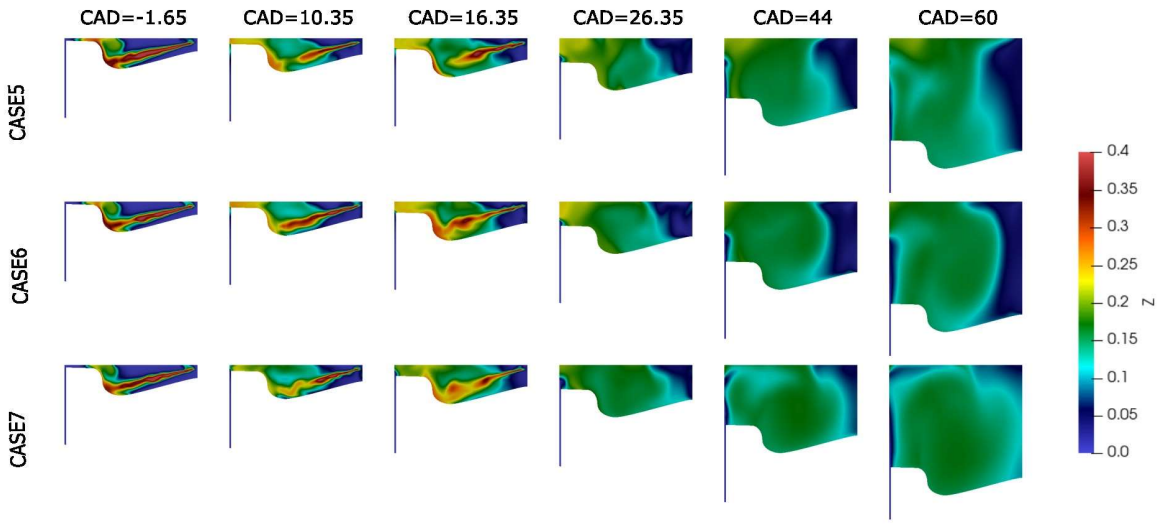

Figure 4.18 Mixture-fraction 2D-contour for the hole number study.

In Figure 4.19 the maps of the equivalence ratio in function of the temperature are shown, as mentioned in section 2.3 the equivalence ratio is the ratio of the actual ratio of fuel to air divided by the stochiometric fuel to air ratio. We see two dashed lines showing us the soot and NOx-limit. The soot-limit starts at the higher equivalence ratio (richer) and expands further as the equivalence ratio rises because soot is formed more when there is an incomplete combustion because of the higher amount of carbon-rich particles. For all three figures we basically all work under the soot limit. The NOx-limit is seen from higher temperatures and the region spreads more as the temperature increases, this region is also in the lower levels of equivalence ratio (leaner). This is due to NOx's being formed at higher temperatures and when enough oxygen is present.

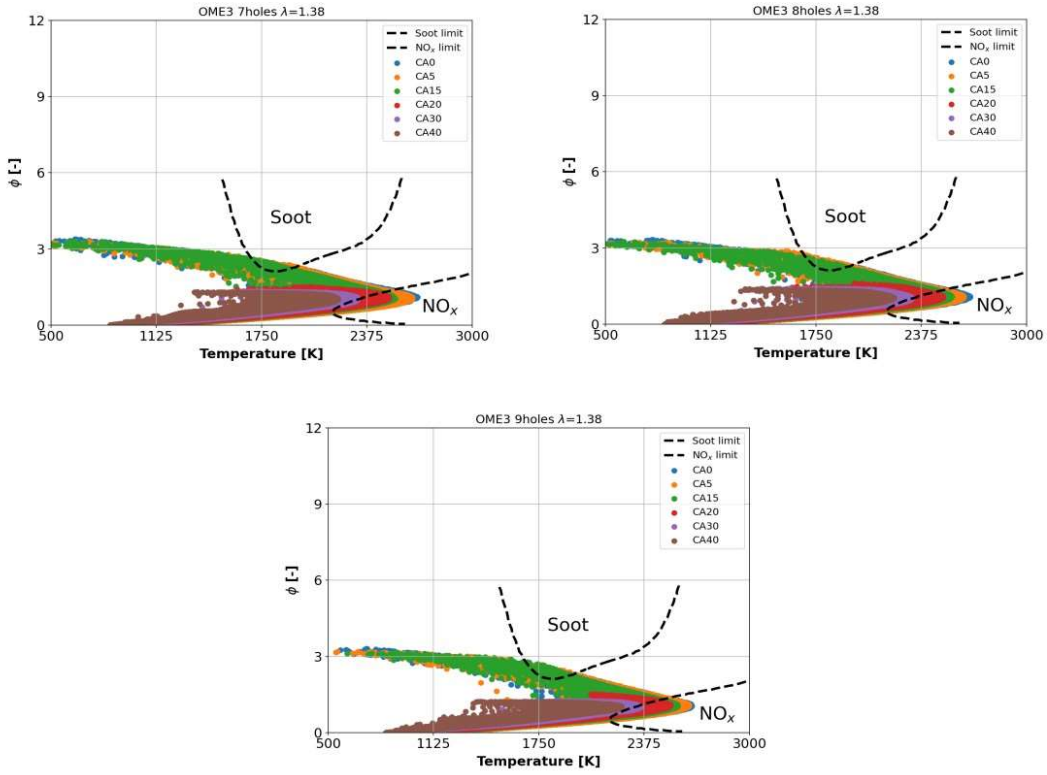

Figure 4.19 Phi in function of temperature plot comparison for the hole number study.

When an internal combustion engine is equipped with an injector with more holes it is possible to obtain a better performance in terms of combustion efficiency as seen in Figure 4.20 because the hole diameter is smaller, which provides smaller fuel droplets resulting in a better atomization and evaporation of the fuel. This can be concluded for the cases considered, even more than 9 holes could result in worse properties because the fuel sprays could start 'competing' to find the oxygen available in the chamber, which will negatively influence the mixing rate. Also, in general we have a better combustion efficiency for all the OME-cases than for the diesel case. This is due to the OME3-fuel having a higher cetane number as seen in Table 1. The higher combustion efficiency than reduces the emissions. [43], [44]

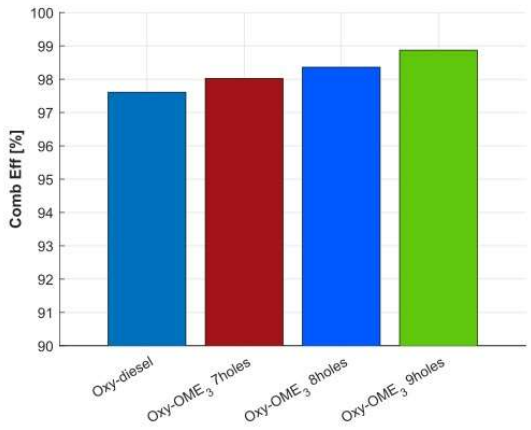

Figure 4.20 Bar-chart of the combustion efficiency for the hole number study.

In the graph in the upper left corner in Figure 4.21 for the hydrocarbons, although a higher value than the diesel case, the lowest value can be seen for the 9 holes case. The other OME-cases with 7 and 8 holes have bigger nozzle-diameters, which result in higher HC emissions because of a worse evaporation and air-fuel mixture due to a poor atomization. A positive aspect is that for the case with 9 hole orifices we come pretty close to reaching the same level of HC as for diesel. [37], [40]

The incorrect conclusion can be drawn from the soot bar chart in Figure 4.21's lower left corner where there is significantly more soot observed in the case with nine holes. But if a look is taken at the magnitude of the unit of 10^{-20}, the soot is practically non-existent.

In the top left corner of Figure 4.21 the last values of the hydroxyl-content are given. Previously the course the concentration follows over the crank angles has been discussed with the reasons of why the 9 holes case has the lowest last value. Moreover, we discussed the reason of oxy-diesel having the highest last value but this could be inaccurate and has to be further conformed with the experiments.

In the bottom right corner, the carbon monoxide concentration is given in Figure 4.21, a decrease in carbon monoxide concentration can be seen in relation to increasing the number of injector holes. This is due to the better utilization rate of the oxygen when increasing the amount of injector holes due to the better evaporation and atomization of the fuel. Also, the carbon monoxide concentration is way lower for the OME-cases than for the diesel case. Another reason for the decrease of carbon monoxide when increasing the number of orifices, is the increased temperature we see in Figure 4.1. The increase in temperature makes sure more CO is further oxidised into CO_2.[40], [45]

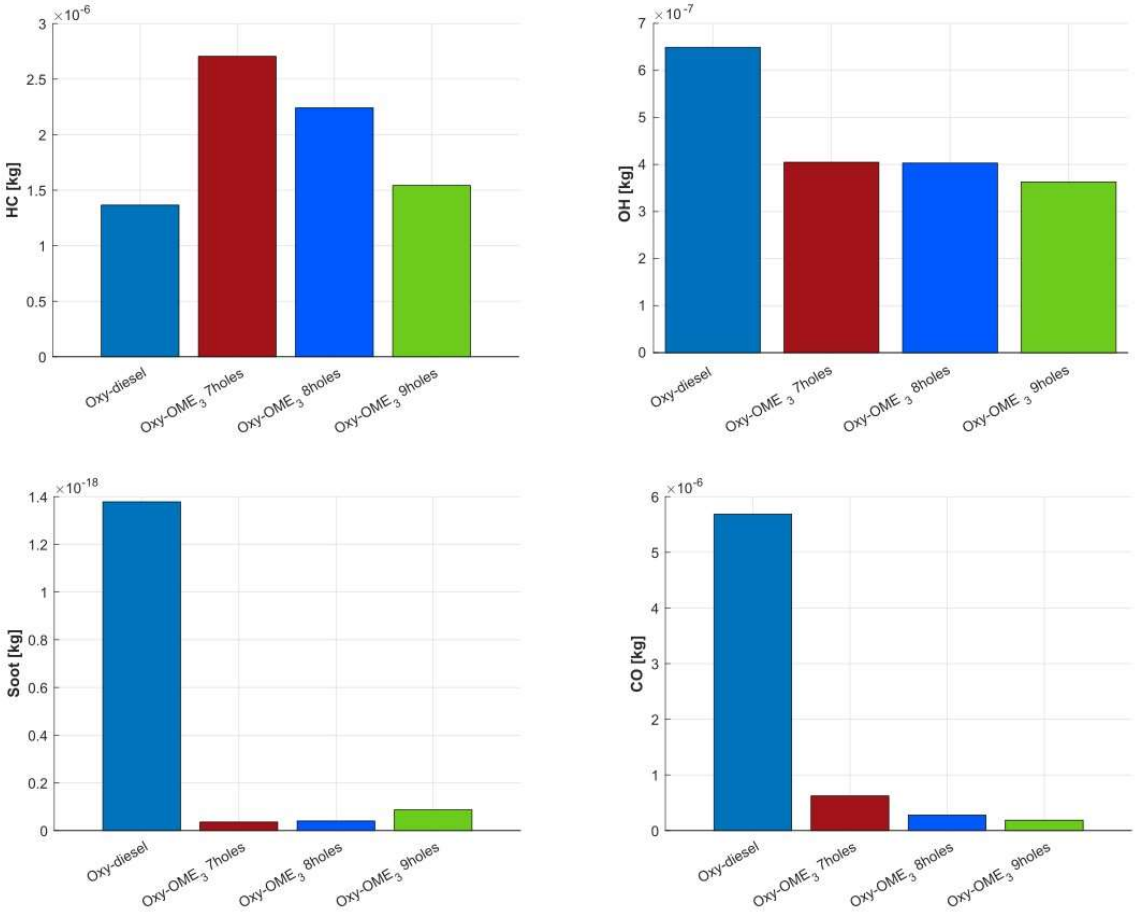

Figure 4.21 Bar-chart of the pollutants for the hole number study.

Other important properties we are plotting in Figure 4.22, are bar-chart for is the indicated mean pressure (PMI) and the Indicated Specific Fuel Consumption (ISFC). For the PMI we see a higher value for all the cases using OME_3-fuel compared to diesel, with the highest value being at case seven. A higher value of PMI is favourable because this means more force is exerted on the piston during the expansion stroke resulting in a higher engine performance and efficiency. We do have to take in mind that a higher PMI results in more engine wear and can drastically affect the engine-life. PMI is one of the most relevant parameters to assess a combustion process, a higher PMI is generally correlated with a higher combustion efficiency.[46]

If we make the comparison for the ISFC, as seen that changing to OME_3 as fuel has a negative impact on the amount of fuel being used. More fuel is consumed to create a given power output since the LHV is much lower for OME3 than for diesel. Although changing the number of injector holes the ISFC is similar for the three OME-cases, since the same amount of fuel is inserted in all three cases. [45]

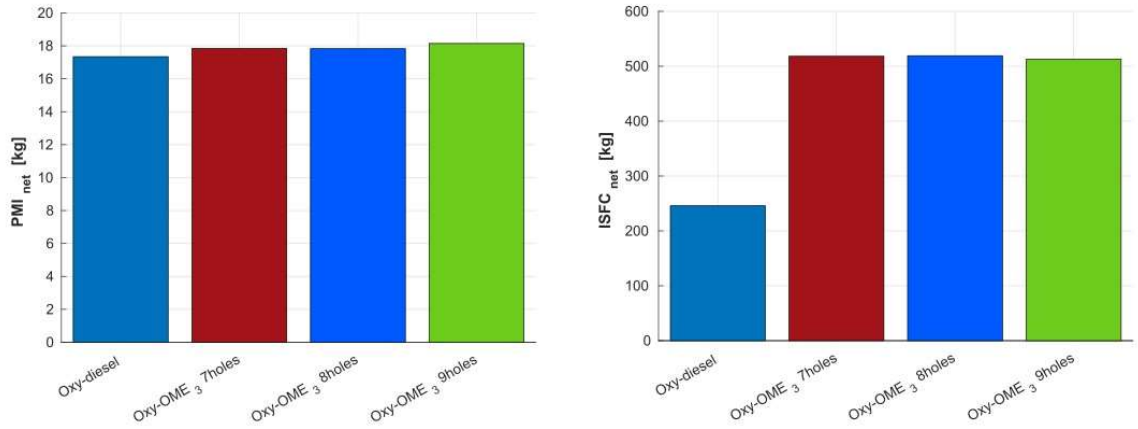

Figure 4.22 Bar-chart of the indicated mean pressure and the indicated specific fuel consumption for the hole number study.

4.1.2 Iso-lambda comparison

- **Thermodynamic comparison**

In the Iso-lambda comparison, we occasionally include the "Vemod"-case for further analysis an evaluation. "Vemod" is a Virtual Engine Model, its use is in simulating engines and the one we are comparing with is one created by CMT. An Iso-lambda comparison is useful so the chemical properties and combustion characteristics can be assessed better in a comparison. When looked at the pressure in Figure 4.23, the highest pressure is achieved for the Y_{IVC} case where the concentrations are adjusted. For the temperature graph, the highest temperature is achieved for the T_{IVC} case what was expected because we adjusted this temperature to get the same lambda as the diesel case. When compared to the Y_{IVC} case a certain offset is seen between the two temperature graphs. The start of combustion (SOC) is earlier for both OME-cases than for the diesel case. This trend can be seen again for the point where 90% of the fuel is already burned (CA90).

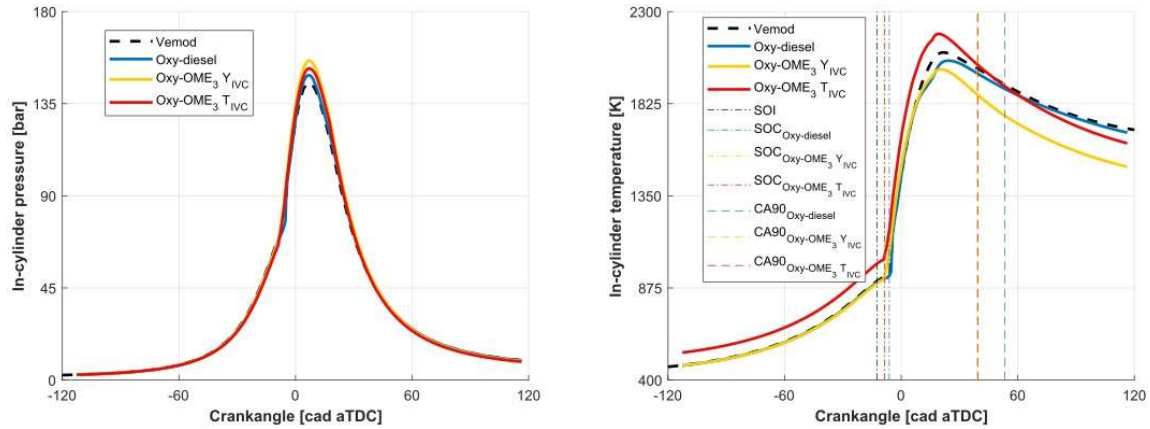

Figure 4.23 Temperature comparison for the Iso-lambda study.

Figure 4.24 shows the temperature contour comparison between the cases diesel, OME_3 adjusting the IVC temperature, and OME_3 adjusting the IVC concentration with the same λ. It is possible to see that the case 9 (adjusting the temperature) presents higher temperatures for the first two crank angles evaluated due to the higher temperature on the start of the simulation. Furthermore, the case 8,

adjusting the concentrations, shows lower temperatures than the other cases because of the concentrations changes affect the amount of trapped mass in the IVC. Moreover, in the same condition the results for the OME_3 simulations shows a faster combustion than the diesel case.

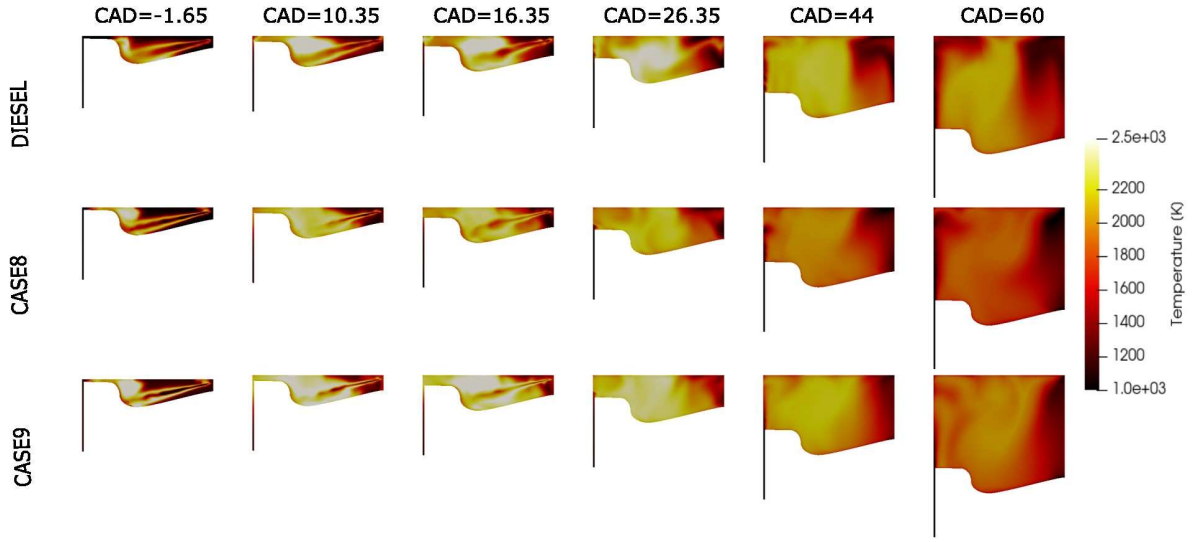

Figure 4.24 Temperature contours comparison for the Iso-lambda study.

In the graphs below in Figure 4.25, the Rate of Heat Release is given for the different cases, one graph full view over all crank angles while the other is the zoom-in view. On the full view a very big is show of 571.8 J at -5 CAD for the Oxy-diesel case and a peak of 121.342 J @-8.6625 CAD for case nine. The peak we see in these graphs is artificial and in the experiments, lower values would be expected so an exaggeration was made during the premixed phase. This higher peak happens due to the differences in LHV, as discussed in 2.6 the LHV represents the amount of heat released when the fuel is fully combusted in normalized conditions of pressure and temperature. So, the LHV of diesel is more than double that of OME (44.5 to 19.6 MJ/kg) which is shown in Table 1. What do can be seen is that the peak happens earlier for both OME cases, this is due to the higher cetane number compared to diesel. The cetane number indicates at what speed the fuel can be combusted, so OME will have a shorter ignition delay during the premixed phase. During the mixing-controlled combustion phase, less heat is released for the oxy-diesel case than that for the other cases because of the excess amount of oxygen in the combustion chamber. Moreover, can be seen that the late stage of combustion is faster for OME than for diesel-fuel because most fuel is already burned during the early stages of the combustion for OME. The trajectory for both OME cases is nearly identical, so during the premixed combustion phase the and the mixing-controlled combustion phase there is overlap. Only during the late combustion phase the Y_{IVC} graph is a bit higher than that of the T_{IVC} case, so more heat is still released during this phase for the Y_{IVC} case this can be due to having some unburned fuel left.

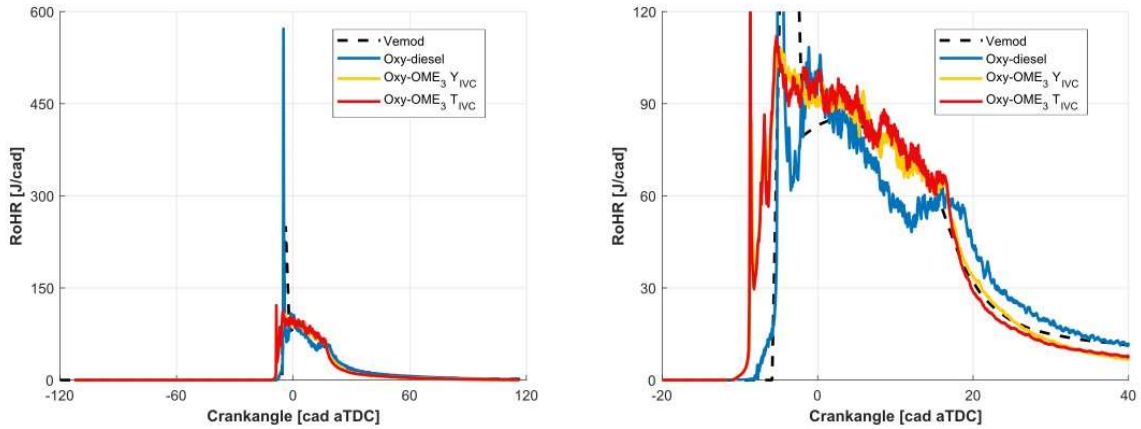

Figure 4.25 Rate of Heat Release comparison for the Iso-lambda study, with the left one being a zoom.

Figure 4.26 presents the normalized cumulative heat release. It is possible to see that all cases are able to consume almost all of the fuel, providing good values for combustion efficiency, and converting the fuel energy in work. For the cases using OME_3 as fuel it was possible to reach higher values than the other cases because the combustion is faster for this fuel.

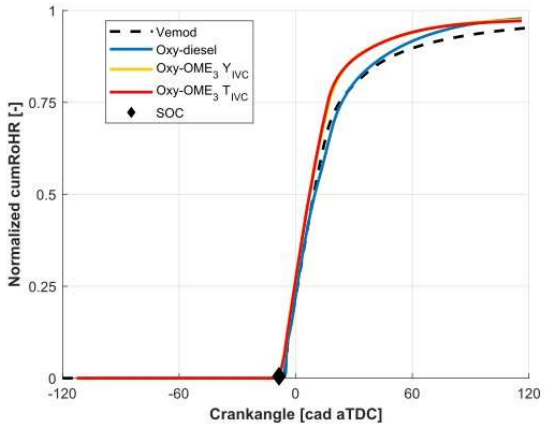

Figure 4.26 Cumulative Rate of Heat Release comparison for the Iso-lambda study.

In Figure 4.27, the gamma value (*γ)* is shown, also called the heat capacity ratio. This ratio has a high temperature dependency, the higher temperature results in a lower value. This can be recognized in the graph since T_{IVC} has the lowest gamma value over all crank angles. In general the Y_{IVC} curve lays beneath the oxy-diesel curve, except for after 60 CAD due to the temperature dependency and the oxy-diesel having the highest temperature at the last crank angles in Figure 4.23. Gamma is also dependent on the air-fuel mixture, a higher lambda would mean that the curve translates more to the top right corner. Since, the OME fuels have a lower lambda than we would normally have when we just change the fuel from diesel to OME without changing the conditions, the graph will move more to the bottom left corner. This lower value of heat capacity ratio does imply a lower engine efficiency but this might be able to be solved by using different operating conditions. [39]

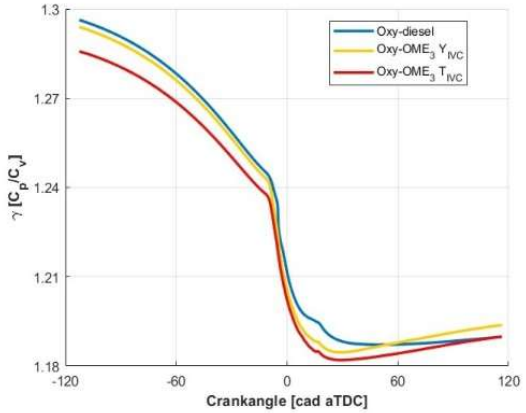

Figure 4.27 Gamma comparison for the Iso-lambda study.

- **Emissions comparison**

For the oxygen concentration the crank angles (-1.65, 10.35, 16.35, 26.35, 44 and 60) were chosen, these can be recognized in Figure 4.28 by the vertical dashed lines. Over all crank angles the graphs of the T_{IVC} and Y_{IVC} are exactly overlapping. This is due to the same lambda and the same fuel being used, normally if there is being changed to OME-fuel from diesel without changing any boundary conditions a lambda of 1.38 would be achieved instead of 1.21 which causes the graph to translate higher up. Now there is being worked on conditions that are leaner resulting in a translation of the graphs using OME_3 as fuel downwards. Now there is too little excess oxygen for the OME to be burned efficiently resulting in the worse combustion efficiency which we will see later on, that's why the oxy-diesel graph dips relatively deeper than the OME-cases nearly surpassing it. If there was being looked at a concentration graph, the graphs of Oxy-diesel and T_{IVC} would overlap until the start of injection since they have the same concentrations at IVC. But when this is converted to kg, a lower value appears due to the higher temperature resulting in a lower density and thus a lower mass trapped in the cylinder.

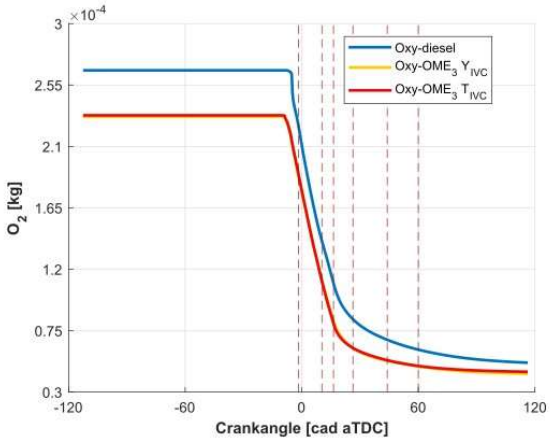

Figure 4.28 Oxygen-content comparison for the Iso-lambda study.

The *paraView* contours in Figure 4.29 were created at the same crank angles as mentioned above, during the creation of these contours a threshold value of 0.1 was used. Over all crank angles we see a higher amount of oxygen in the combustion chamber for the diesel case. Especially during the first

crank angle of -1.65 there is way more oxygen available than for the OME-cases, the reason for this is the longer ignition delay for diesel because of the lower cetane number. A shorter ignition delay the oxygen is burned later during the first stage of combustion. For the crank angles -1.65, 10.35 and 16.35 we do see a lot lighter colours for the Y_{IVC} case (case 8), but based on previous Figure 4.28 the total mass of oxygen should be the same for both OME-cases just the concentrations are higher for the T_{IVC} case since the starting concentration of oxygen at IVC was 0.3103 instead of 0.273 for the Y_{IVC} case. Looking at all crank angles higher than -1.65, the way the oxygen concentration can be seen. The concentration is based mostly in the middle of the cylinder, and at the crevice while the oxygen is consumed in the direction of the spray.

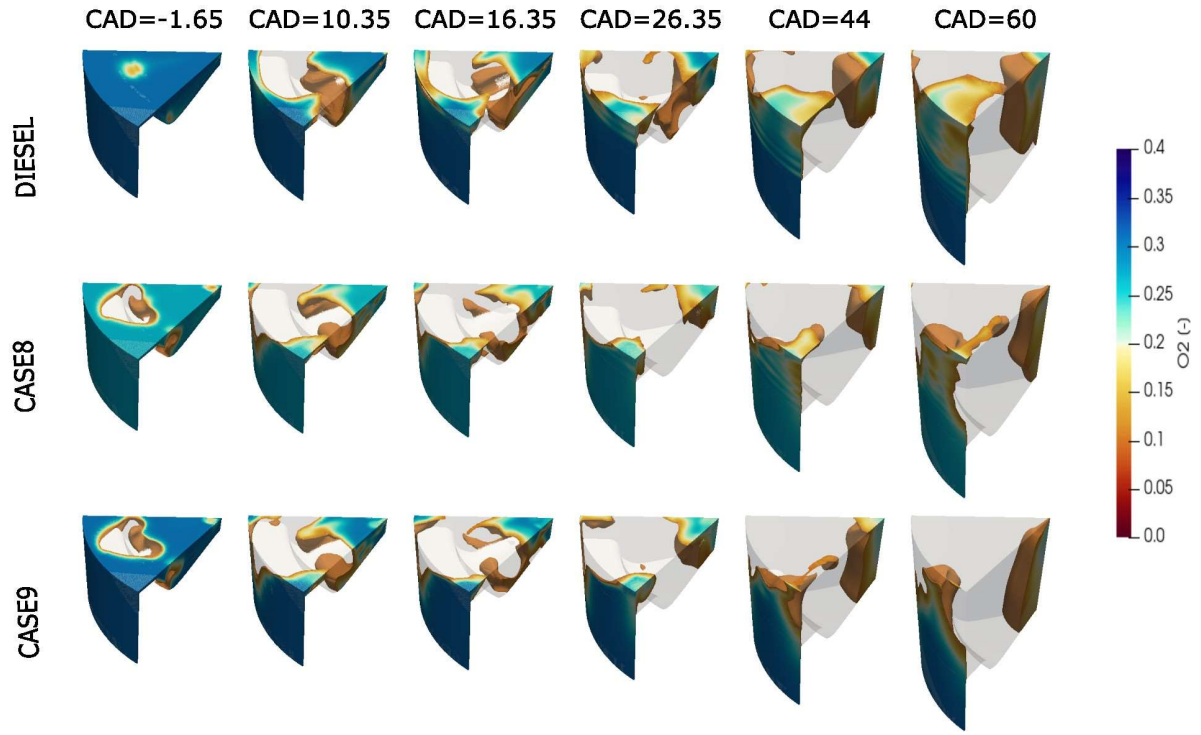

Figure 4.29 Oxygen-content 3D-contours comparison for the Iso-lambda study.

In Figure 4.30, the different carbon dioxide contents are given at the same crank angles as mentioned above and shown as the vertical red dashes lines. The highest content of carbon dioxide is seen for the Y_{IVC} case since the concentration at IVC is higher (0.4481 instead of 0.4294). From IVC to SOI, the Oxy-diesel case and the T_{IVC} will have the same concentrations but since the T_{IVC} case has a higher temperature when the intake valve is closed the mass will be lower because of the lower density. However, because of the excess amount of oxygen in the OME-fuels the mass of carbon dioxide will be higher for the Y_{IVC} case. Also, the slopes of both the OME-cases are steeper since this fuel burns faster, creating the main combustion products faster. However as the concentrations of CO_2 both will

be higher for OME and have the same values at the end of combustion than for oxy-diesel, again the mass will be lower because of the temperature.

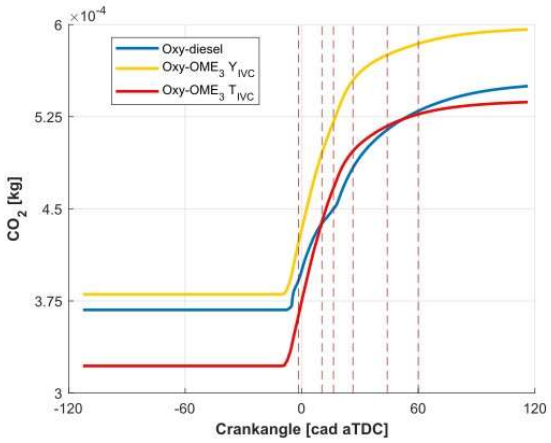

Figure 4.30 Carbon dioxide-content comparison for the Iso-lambda study.

In Figure 4.31 the contours for carbon dioxide were created in *paraView* with a threshold of 0.45. At -1.65 CAD the highest concentration can be seen for the Y_{IVC} case (case 8) while further into combustion the concentrations for both OME-cases stay about the same since using the same lambda value and having the same fuel properties. Where diesel has lower CO_2 concentrations over all crank angles because diesel doesn't have any oxygen in its structure, the diesel case will have more byproducts such as carbon monoxide while the OME-fuel manages to form CO to CO_2. [47]

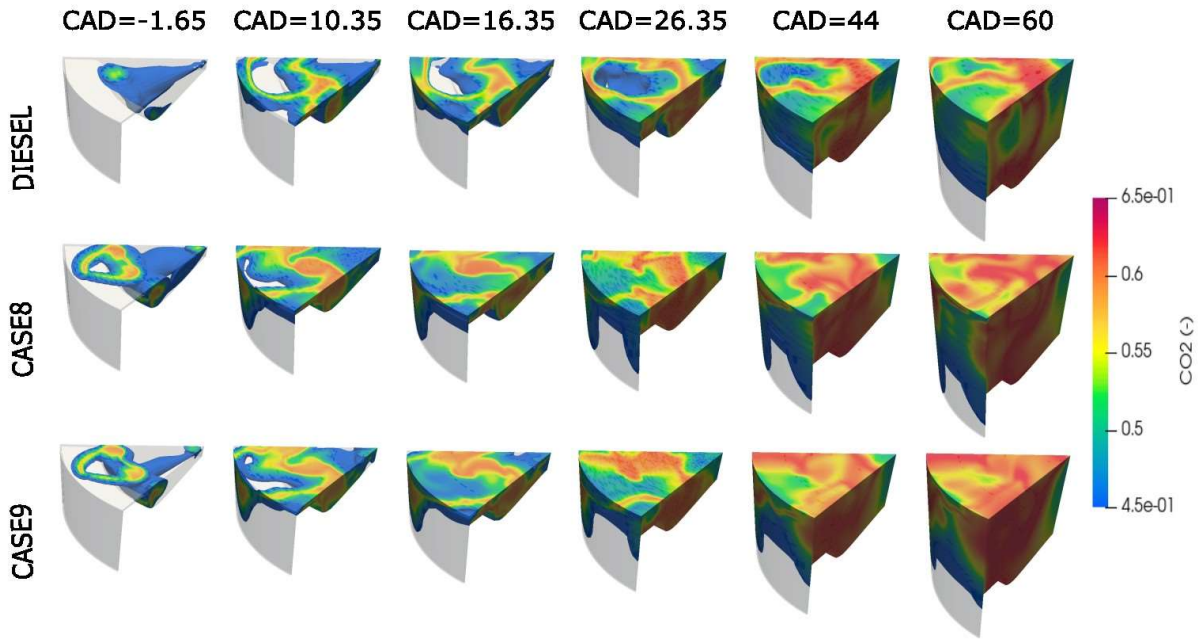

Figure 4.31 Carbon dioxide-content 3D-contours for the Iso-lambda study.

Just like in the number of injector holes comparison a much higher value of C_2H_2 is presented in Figure 4.32 for the diesel case since it does have carbon-carbon bonds and OME does not. This once again conforms to the non-sooting nature of OME_3, since C_2H_2 is evaluated because it is the soot emission precursor.

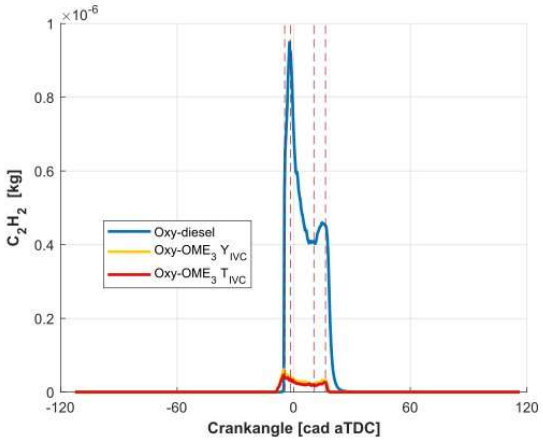

Figure 4.32 Acetylene-content comparison for the Iso-lambda study with the diesel case.

In Figure 4.33, the diesel case has been excluded from the comparison and a zoom was made. Higher levels of acetylene were achieved over all crank angles for the Y_{IVC} but since these values are in the order of 10^{-8}, these values can be expected negligible.

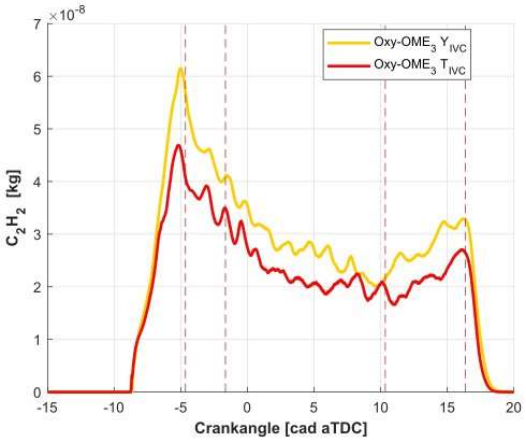

Figure 4.33 Acetylene-content comparison for the Iso-lambda study.

The 3D-contours for the acetylene in Figure 4.34 are chosen over a broad crank angle range which is actually not needed since these soot precursors are only formed during a very small part of the combustion process. Therefore, only the crank angles -1.65, 10.35 and 16.35 will be considered and a threshold 1.7e-12 will be used. In the pictures there can be recognized that for crank angles higher than 16.35, the C_2H_2 is declining for all three cases, especially for the OME-cases where only C_2H_2 concentration is left in the middle of the geometry and at the cylinder walls.

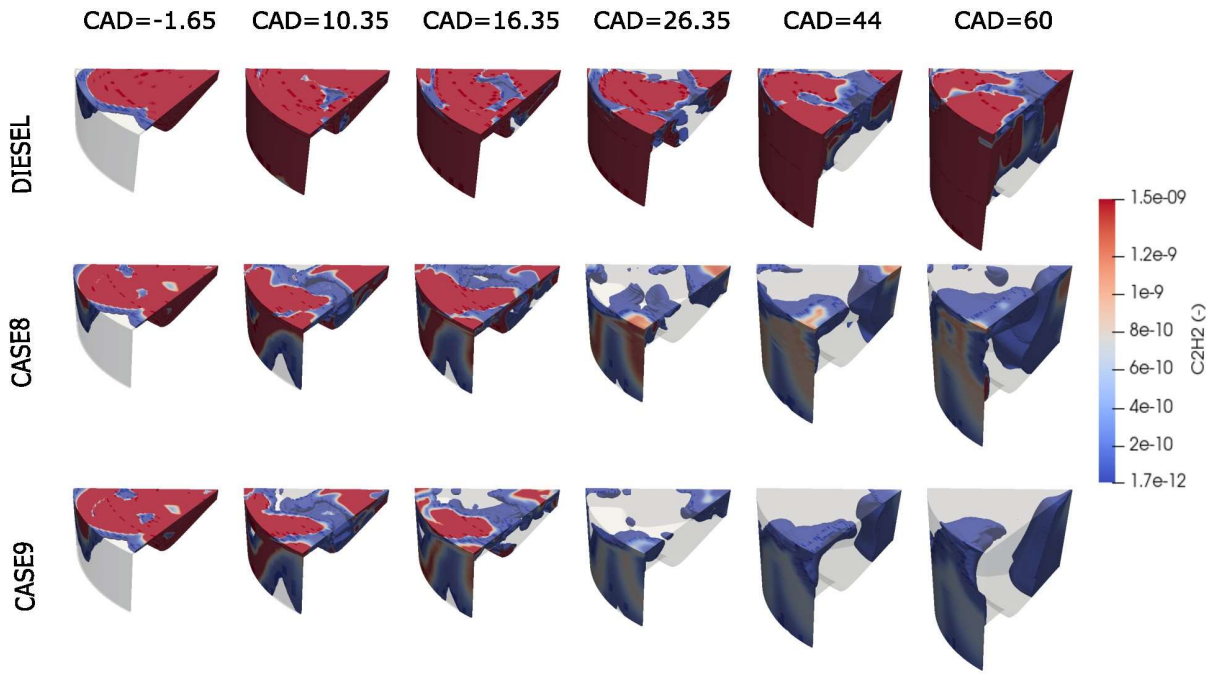

Figure 4.34 Acetylene-content 3D-contours comparison for the Iso-lambda study.

In Figure 4.35 the analysis of the hydroxyl content is shown over a broad range of crank angles (-1.65, 10.35, 16.35, 26.35, 44 and 60), the same crank angles will be used to create the contours. The Y_{IVC} case has the highest OH-formation over all crank angles because of the higher temperature and since OH is a good tracker for high temperature oxidation reactions. Due to working in more lean conditions there is less OH formation for OME in general because there is not such an excess of oxygen available as in the number of holes comparison where for all three OME-cases a higher hydroxyl-content was achieved compared to diesel. [28]

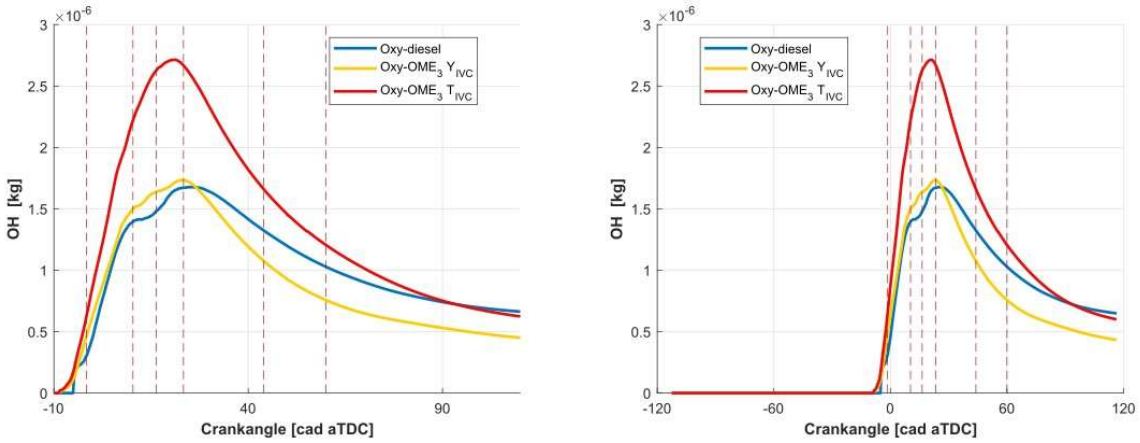

Figure 4.35 Hydroxyl-content comparison for the Iso-lambda study, with the left being a zoom.

For all the three cases, as can be seen in Figure **4.36** most of OH-content is concentrated in the bowl of the piston and less on the inside. What is also very noteworthy, is the difference between the hydroxyl concentration of the Y_{IVC} and the T_{IVC} case, it is way lower for the Y_{IVC} case. It is even lower than that of the diesel case in contrary to our expectations as the oxygen-content in the OME-fuel

could lead to a higher oxidation rate of the fuel. Hydroxyl is seen as a tracker for oxidation reactions at high temperature, that is why the higher temperature in the T_{IVC} case leads to more OH-formation. [28]

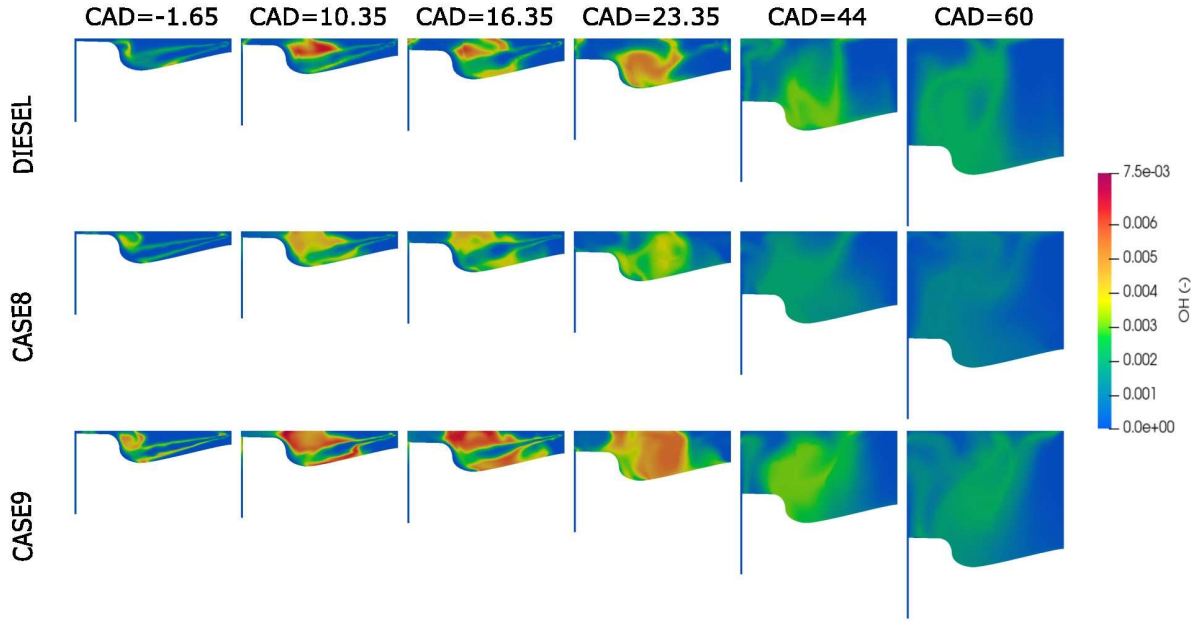

Figure 4.36 Hydroxyl-content contour for the Iso-lambda study.

- **Global engine analysis**

The first parameter talked about in the global engine analysis is the total cylinder mass distribution shown in Figure 4.37. The figure shows the total cylinder mass for all three cases over three relevant equivalence ratios. One ratio represents the more stoichiometric condition (mt>1.05), another represent lean condition (mt>0.55) where there is a deficit of fuel and the last one represent rich condition (mt>1.75) where there is an abundance of fuel. Directly can be seen that both the OME-cases work in more lean conditions than the diesel case as is previously discussed since there is being worked at lambda values lower than usual. The case with the leaner conditions is the Y_{IVC} case since at IVC it has the lowest O_2-concentration (0.273 instead if 0.3303). The diesel case works mostly in rich and stoichiometric mixture while it is not able to consume all the all the mass in this condition, which it does in rich conditions. Both OME-cases also have a similar trend in both rich and stoichiometric conditions, with in stoichiometric conditions just not being able to consume all mass.

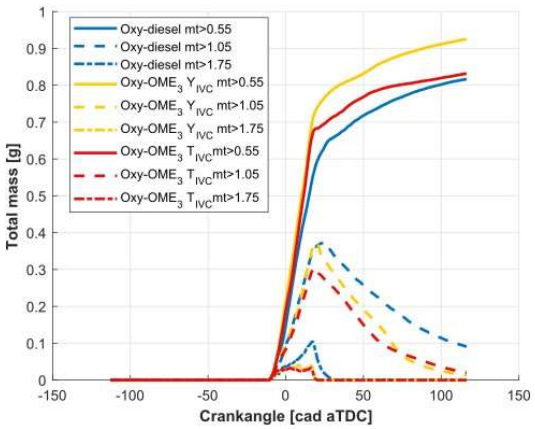

Figure 4.37 Total cylinder mass distribution comparison for the Iso-lambda study.

In Figure 4.38 the mixture fraction is chosen at crank angles (-1.65, 10.35, 16.35, 26.35, 44 and 60). Immediately at crank angle of -1.65 the differences in spray between the OME and diesel cases catch the eye with the OME spray being way more penetrating and consisting out of way less red (less fuel). In the following crank angles of 10.35 and 16.35 the fuel gets way more distributed over the bowl for the OME cases while the spray is still prominently visible, in contrast to the diesel case where the fuel is mostly concentrated in the curve of the bowl. The following crank angles a deficit of fuel is seen in the middle of the geometry for all the cases but it stands out the most for the diesel case where in a big part of the there is no fuel.

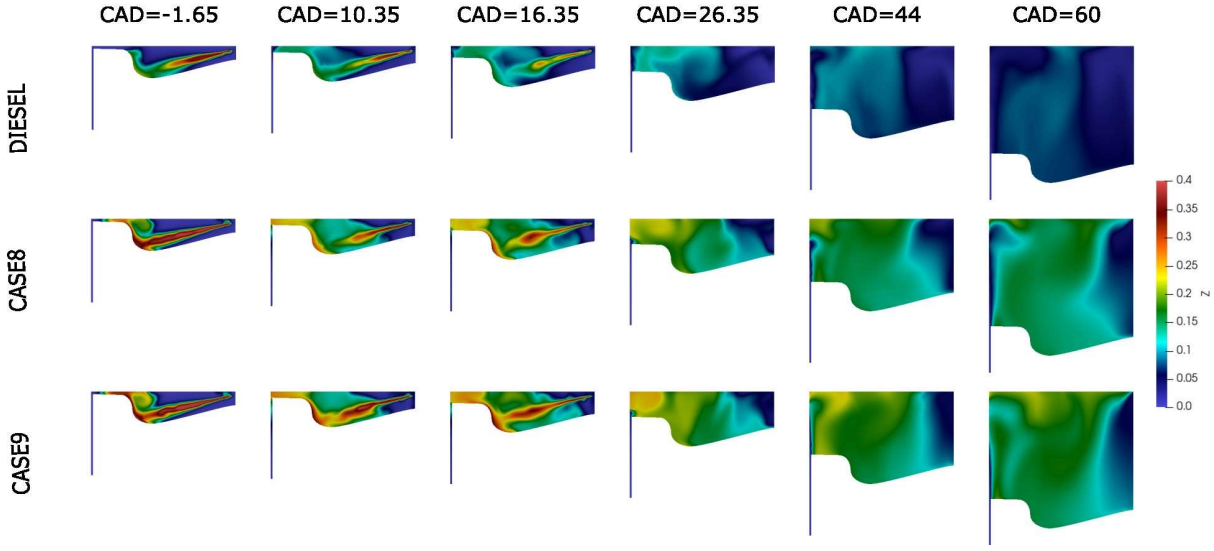

Figure 4.38 Mixture-fraction 2D-contour for the Iso-lambda study.

Looking at Figure 4.39 the equivalence ratio graph in function of the temperature can be seen for the reference diesel case. This graphic shows a larger equivalence ratio field for diesel when compared to the other OME examples of the Iso-lambda comparison. In general we see lower equivalence values for OME-fuel over all crank angles especially for the lower crank angles (CA0, CA5 and CA15), the OME-fuel works in more lean conditions. This is due to the reactivity of OME that we can still have combustion even on very low equivalent ratio values. There are also many points within the soot limit

for the diesel case, which is not so for the OME cases. The OME-cases enter the soot limit only for a small amount of points and for low crank angles as CA5 and CA15. Diesel also enters the soot limit for all the higher crank angles. For the NOx-limit, more points are just touching the limit while for the OME-fuels more enter the limit, this is not a major concern as oxy-fuel combustion is used here. The reason that more NOx is formed is because with OME-fuel there is a surplus of oxygen and so more lean conditions are employed. This introduces more opportunity to oxidise the nitrogen that would be present had air been used. [28]

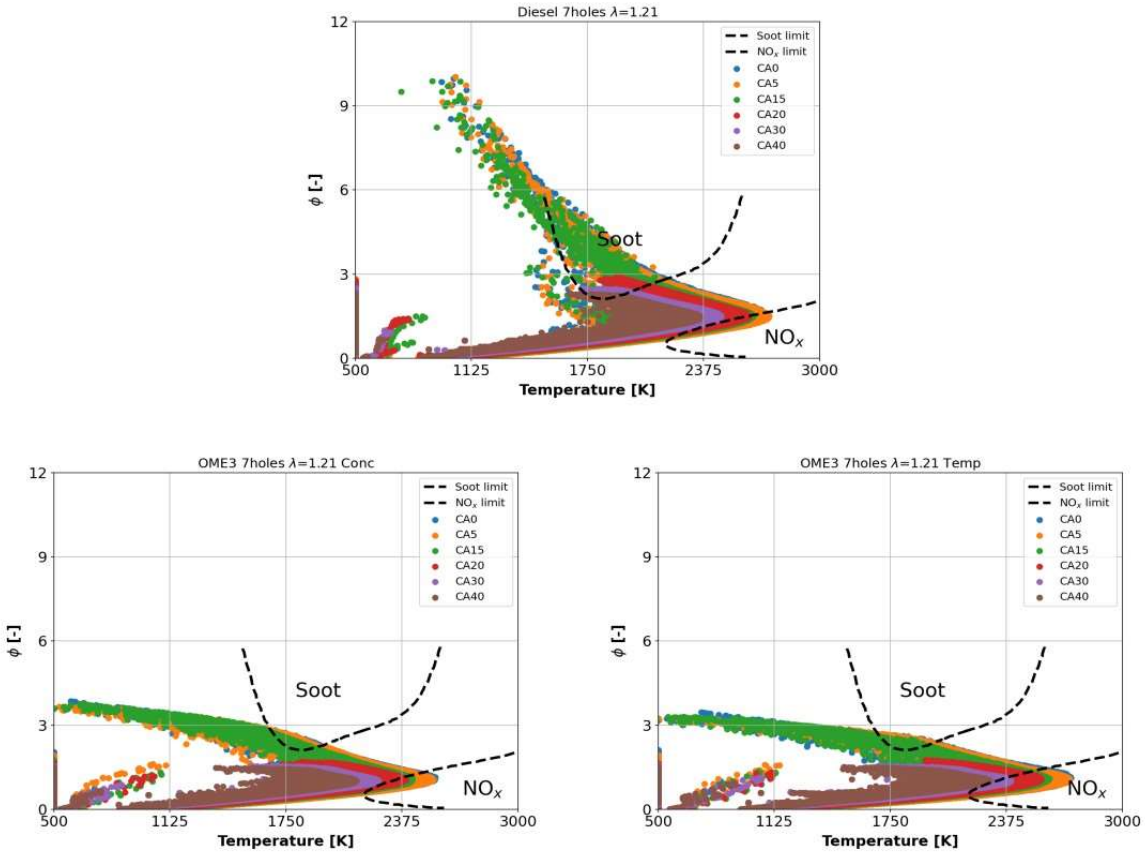

Figure 4.39 Equivalence ratio in function of temperature plot comparison for the Iso-lambda study.

In figure Figure 4.40 the combustion efficiencies are shown with diesel having the best efficiency, followed by the Y_{IVC} case and the T_{IVC} case. In the contrary to which we saw in the previous comparison where the combustion efficiency was the lowest for the diesel case. This is due to the lower lambda value now used of 1.21 instead of 1.38, so more rich conditions are used than in previous comparison. Combustion is correlated with the lambda value so a shortage of oxygen results in a worse efficiency. OME_3 having a lower caloric value also contributions to a lower efficiency since more fuel should be injected into the cylinder to get the same energy release. [48], [49]

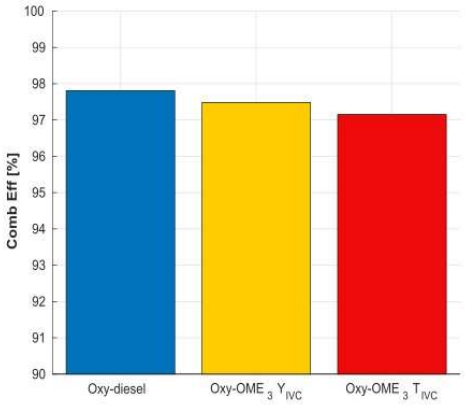

Figure 4.40 Bar-chart of the combustion efficiency for the Iso-lambda study.

In the top left corner in Figure 4.41 the soot is considered for the three cases, for both OME cases it is basically non-existent because of the lack of carbon-carbon bonds in the fuel. There is not even a bar chart to be seen for the T_{IVC} case, a little bar can be seen for the Y_{IVC} case this is due to the higher levels of soot precursor C_2H_2.

In the bottom left corner of the figure amount of hydrocarbons is shown. Both the OME-cases have a higher level of unburned hydrocarbons, with the Y_{IVC} case having the least amount of hydrocarbons of the two. One of the reasons of the lower level of unburned hydrocarbons for the diesel case is the better combustion efficiency.

In the top right corner of Figure 4.41 the carbon monoxide levels are given, directly the oxy-diesel case jumps out with by far the most content. The OME-cases have lower CO-content since the higher levels of oxygen in oxygenated fuels helps to achieve a more complete combustion, so CO is formed to CO_2. One of the reasons why the Y_{IVC} case has less CO than the T_{IVC} case is the better combustion efficiency. [47]

In the bottom right corner of the last value is given for the hydroxyl-content. The T_{IVC} case has the highest hydroxyl-content of the two OME because of the temperature dependency of OH. As previously mentioned in the number of holes comparison, it could be that the OH-content for diesel is not accurate since it is rising at the last crank angles, this has to be checked with the experiments.

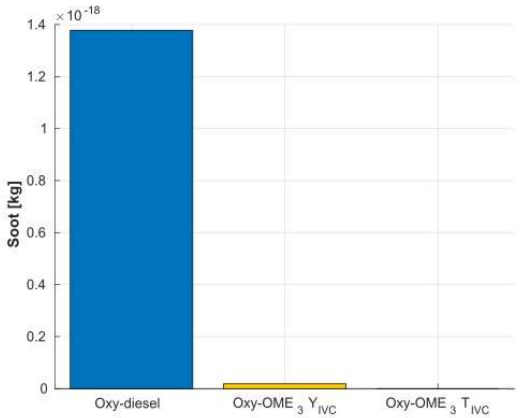

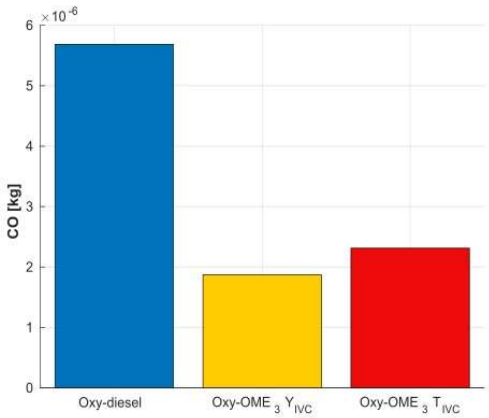

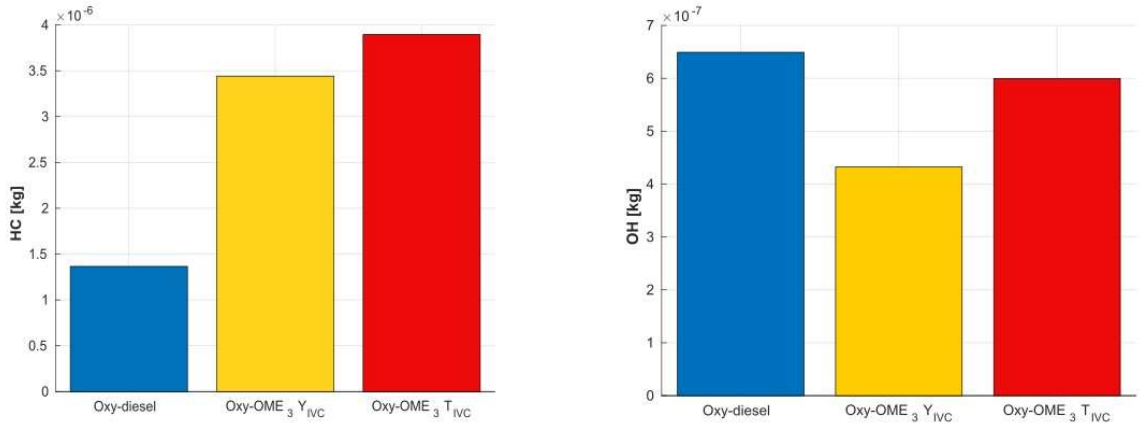

Figure 4.41 Bar-chart of the pollutants for the Iso-lambda study

.

Figure 4.42Figure **4.42** shows us a negative impact of changing to OME-fuel instead of diesel, the indicated specific fuel consumption (ISFC) is way higher. The higher fuel consumption is due to the lower LHV of OME_3. Once it is necessary inject more than twice the fuel to maintain the same amount of energy in the cycle. This aspect could be improved by using blends of diesel and OME_3. The fuel economy is also worse for T_{IVC} case compared to the Y_{IVC} case because of the worse combustion efficiency. For the indicated mean pressure no decisive conclusion could be made since the values are nearly identical. [50]

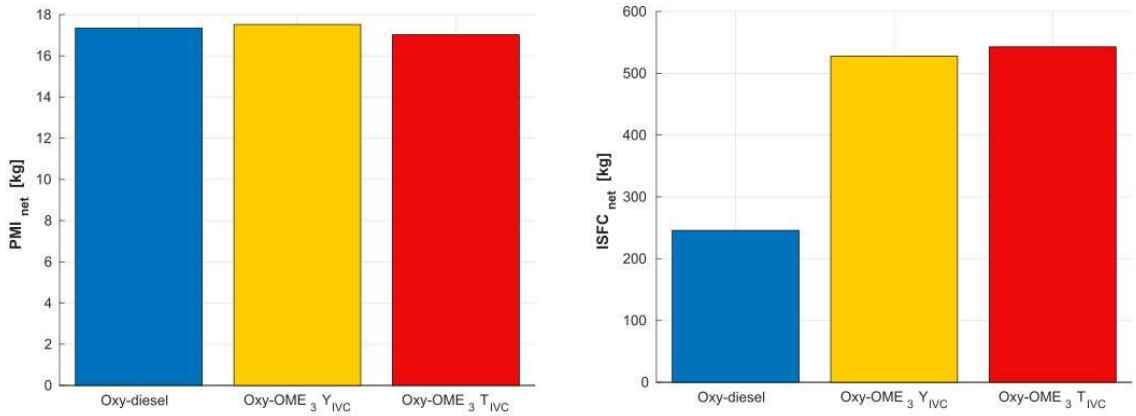

Figure 4.42 Bar-chart of the indicated mean pressure and the indicated specific fuel consumption for the Iso-lambda comparison.

4.2 Decision of the cases

Out of these two comparisons we make a final decision on what is the best option. For this we consider all variables and ultimately decide which would have the most impact. This way we arrive at the most environmentally friendly and efficient option.

4.2.1 Number of injector holes comparison

In general, the best properties were achieved in the 9 holes case. In this case the highest combustion efficiency was achieved with while having less OH and CO-emissions than diesel. Another advantage is that the soot-NOx trade-off doesn't have to be made since there is also no creation of those. The disadvantages are the rise in HC and CO_2-emissions and a worse fuel economy. But since the CO_2-content can be captured and used for other industries or to recreate OME_3-fuel, this doesn't pose any problem. And to better the fuel economy a blend between diesel and OME might be a viable option, this has to be further researched. One thing to keep in mind is that rising the amount of injector holes any further would necessarily result in even better results. Rising the amount of injector holes any further could result in interactions between the different jets. There is a certain threshold for the number of holes, exceeding this threshold leads to worse combustion and emissions due not enough air entrainment so the stoichiometric mixture cannot be achieved. While we changed the number of injector holes we also decreased the diameter size of these holes. The higher velocity of the fuel we receive by having smaller orifices also increase the mixing with air and improve combustion. However, also this shouldn't be changed to very small sizes so that the fuel doesn't move to fast to mix with the air. There are several reasons for needing a higher amount of injector nozzle orifices that have a smaller diameter than that of the diesel case, where 7 holes was the optimal. There are a lot of properties that differ between the fuels for example, OME_3 has a higher viscosity and density. The viscosity effects the performance of the injector and the combustion, the higher viscosity makes for larger fuel droplets. These large droplets result in worse atomization which we can compensate for with the smaller and more injector holes that result in the best configuration. [40], [51]

4.2.2 Iso-lambda comparison

The second comparison where the same lambda was created for the OME-cases as for the diesel case by changing the concentrations and the temperature was not so favourable. The resulting combustion efficiency for both OME-cases is worse than for the diesel case. For the case where the concentrations were adapted (Y_{IVC}), the best properties were eventually achieved. With the best combustion efficiency of the two OME-cases and better CO and OH-emissions than diesel. Also, again no NOx-soot trade off should be made since there is no formation of both. A couple of disadvantages is the worse fuel economy again because of the lower caloric value of OME_3. And the rise in HC and CO_2-emissions, but as mentioned in section 4.2.2, the CO_2 does not pose any problems.

4.3 New case introduction

When a new simulation would be introduced that would come out the best from both comparisons, a case combining case 7 and case 8 would be chosen. This would involve a case with 9 holes and with the concentrations been changed so again a lambda value of 1.21 is achieved using OME_3-fuel. When we finally have simulated this case and it does not come out better than the previous cases, another configuration can be made. Certain parameters are not interchangeable because of the experimental setup, parameters such as the swirl, the geometry of the combustion chamber, the injector itself, the spray angle and the EGR cannot be changed. What we do can change on the setup is the injection

pressure from a range of 1600 bar until 2200 bar, now the optimised setup is using a pressure of 2190 bar. Than we can follow a couple of steps to find the ideal case:

1. Firstly, we use the case seven with 9 holes.
2. Secondly, we change the injection pressure until the ideal one is found.
3. Third we than change the lambda value to the one of the original diesel case in the same way it was done as the best case of the Iso-lambda comparison so by changing the concentrations.

This order could not be followed because of the lack of time, just a case with adapted concentrations for an Iso-lambda comparison and with 9 injector nozzle orifices was composed.

4.3.1 Final configuration

Here the results of the final configuration will be presented. Also there will be assessed if the final configuration which is a combination of the case with most injector holes and the case where the concentrations are changed to achieve the same lambda as in the diesel case, has better properties than the cases separately. In the previous analysis the influence of the number of injector holes on the combustion process has been assessed, that is why in this analysis this last case will only be plotted against the diesel case and the case with changed concentrations.

Table 5 Properties of the last configuration with changed concentrations and 9 injector holes.

	Case 10
Number of Holes	9
Diameter [µm]	165
Amount of fuel [mg/cc]	136.7
Lambda	1.21
SOI [CAD]	-12.4
T(IVC)[K]	474.6
P(IVC)[Bar]	2.58
O_2 -concentration (IVC) [-]	0.273
H_2O-concentration (IVC) [-]	0.2789
CO_2-concentration (IVC) [-]	0.4481
Mass(IVC) [kg]	0.000856
SOI_P [Bar]	58.90
SOI_T [K]	899.42
SOC [CAD]	-8.59

- **Thermodynamical comparison**

In Figure 4.43, the in-cylinder pressure and temperature are assessed. For the in-cylinder pressure the highest pressure is achieved for the case where both the number of injector orifices and the concentration were adapted. The highest temperature is also reached by this case and this peak temperature is reached a bit before the oxy-diesel case reaches its peak. Even though the SOC for

both OME-cases is similar, the case with 9 injector holes has reached the “CA90” point earlier, meaning that the fuel burns faster for this case. This is due to the better evaporation and atomization that come with smaller fuel droplets because of the smaller injector nozzle orifices as mentioned in the number of injector holes comparison. The number of injector holes also leads to a better spread of the fuel, all of these factors lead to faster burning of the fuel resulting in higher in-cylinder pressure and temperature.

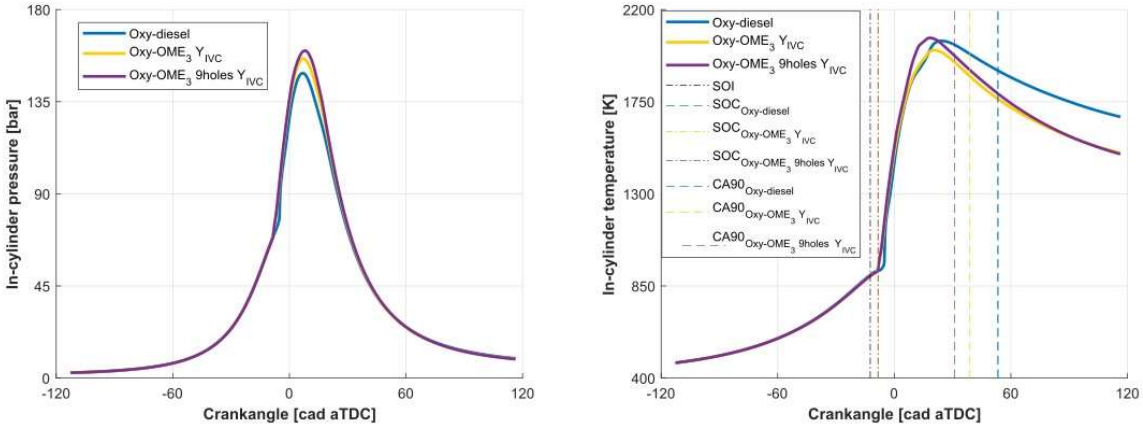

Figure 4.43 In-cylinder pressure and temperature comparison for the study of the final configuration.

In Figure 4.44, the temperature contours are assessed over the crank angles (-1.65, 10.35, 16.35, 26.35, 44 and 60). When looked at the crank angle -1.65 the highest temperature at the end is seen for the case with adapted concentrations (case 8). But from all other crank angles on, a higher temperature is seen for the diesel case since there is more bright yellow in the contours. Although, for the diesel case the temperature is very concentrated while the temperature is more distributed for the case with changed concentrations and 9 injector holes (case 10), which is more favourable since more mixture has the needed temperature for the late combustion. The peak from the in-cylinder temperature for case 10 in Figure 4.43 cannot be recognized in the contours. The reasons for this better temperature distribution for case 10 is again the better atomization and evaporation.

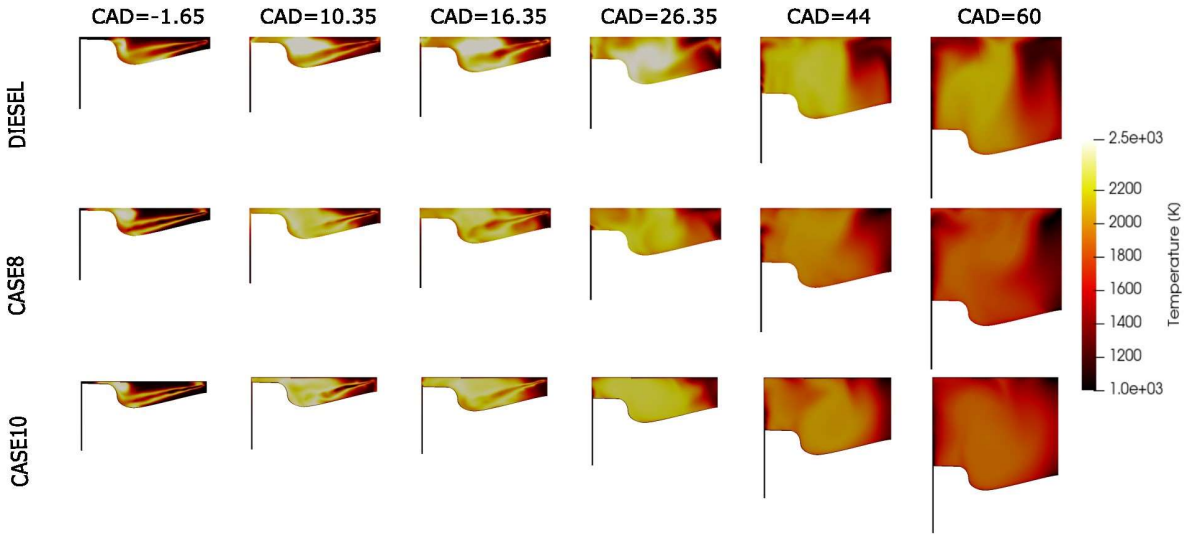

Figure 4.44 Temperature contours comparison for the final configuration.

In Figure 4.45, the rate of heat release is plotted as a wide view and a zoomed view. Immediately the shorter ignition delay for both OME-cases can be recognized compared to diesel. In the following phase (the premixed combustion phase), the peak of the RoHR is formed. The highest peak is achieved for the 9 holes case with Y_{IVC} conditions, better evaporation and atomization will result in higher concentrations of mixture which will burn faster causing a more rapid release of heat, this phase lasts until a minimum is achieved again. The next phase is the mixing controlled combustion, here newly injected fuel starts to burn because of the high temperature mixture. Again the 9 holes Y_{IVC}-case comes out as most favourable since there is a higher energy release with a faster combustion than both other cases.

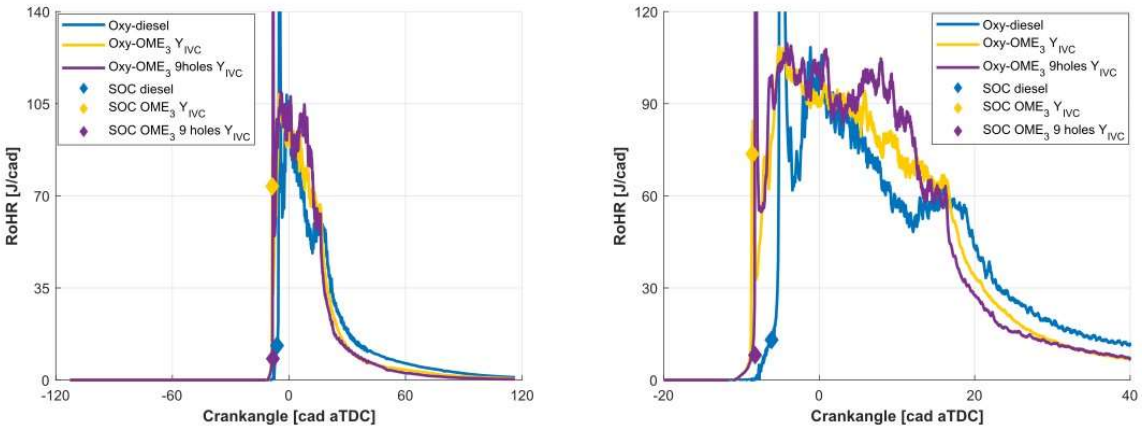

Figure 4.45 Rate of Heat Release comparison for the study of the final configuration, with the right one being a zoom.

Figure 4.46 presents the cumulative rate of heat release which shows how much energy in the fuel got converted into work. For all three cases there can be seen that the graphs approach 100% at the last crank angles, meaning that nearly all energy in the fuel got converted. However, the 9 holes Y_{IVC} case result in a bit higher values of normalized cumRoHR exhibiting a more complete combustion and better combustion efficiency. Also, during the combustion process higher values of cumRoHR are reached faster because of the more rapid heat release.

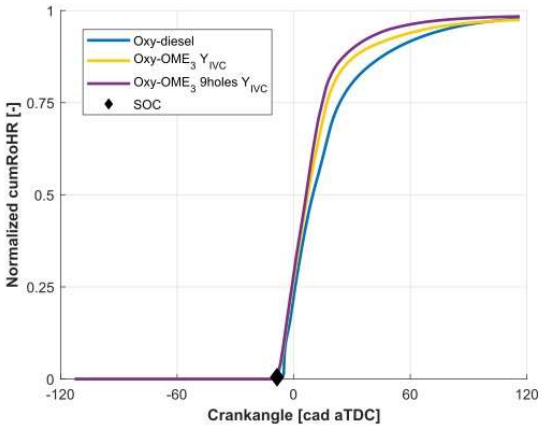

Figure 4.46 Cumulative Rate of Heat Release comparison for the study of the final configuration.

In Figure 4.47 we still have the less favourable (lower) heat capacity ratio than for the diesel case. Since the ratio is temperature and composition dependent and we only added more injector orifices, the heat capacity ratio became even less favourable because of the higher and faster temperature peak of the case with adjusted concentrations and 9 injector holes. Although this lasts until 60 CAD because than the oxy-diesel has a much higher temperature than the two other cases. A lower heat capacity ratio in general would imply a lower engine efficiency but as we will later see the improvements in evaporation and atomization result in a highest combustion efficiency for the 9 holes Y_{IVC} case.

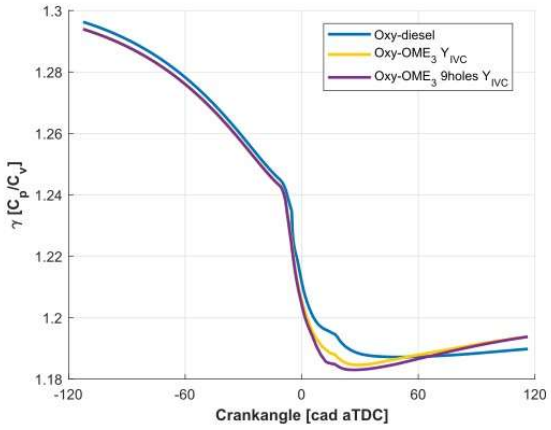

Figure 4.47 Gamma-value comparison for the study of the final configuration.

- **Emissions comparison**

Now, the emissions of the comparison will be assessed. Since in previous comparison (iso-lambda) the differences between the oxy-diesel case and the Y_{IVC} were already discussed we will mainly focus on the 9 holes Y_{IVC} case. The course of the graphs in Figure 4.48 of both OME-cases is similar except from around crank angle 10.35 on, the case where also the number of injector holes were changed dips deeper. This is because more oxygen is being used during the combustion process because we have a more complete combustion process.

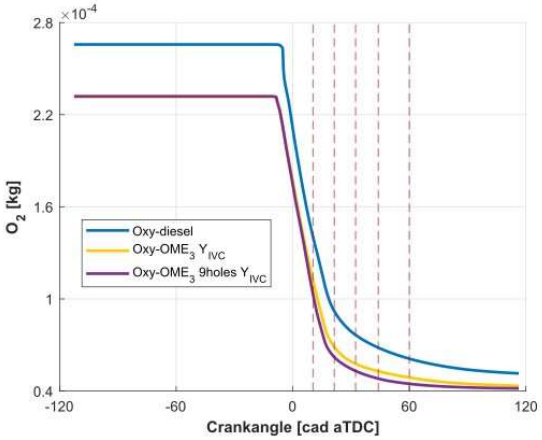

Figure 4.48 Oxygen-content comparison for the study of the final configuration.

In Figure 4.49 the oxygen contours were plotted with a threshold value of 0.1 and at crank angles (-1.65, 10.35, 16.35, 26.35, 44 and 60). At the first crank angle the highest concentrations are seen for the diesel case since it also has higher starting concentrations, while at this crank angle both OME-cases are similar. Looking and the concentration evolution on higher crank angles very similar concentrations are seen for case 8 (Y_{IVC}) and case 10 (9 holes Y_{IVC}) can be seen, but case 10 has a little lower concentrations because of the better oxygen usage during the combustion process.

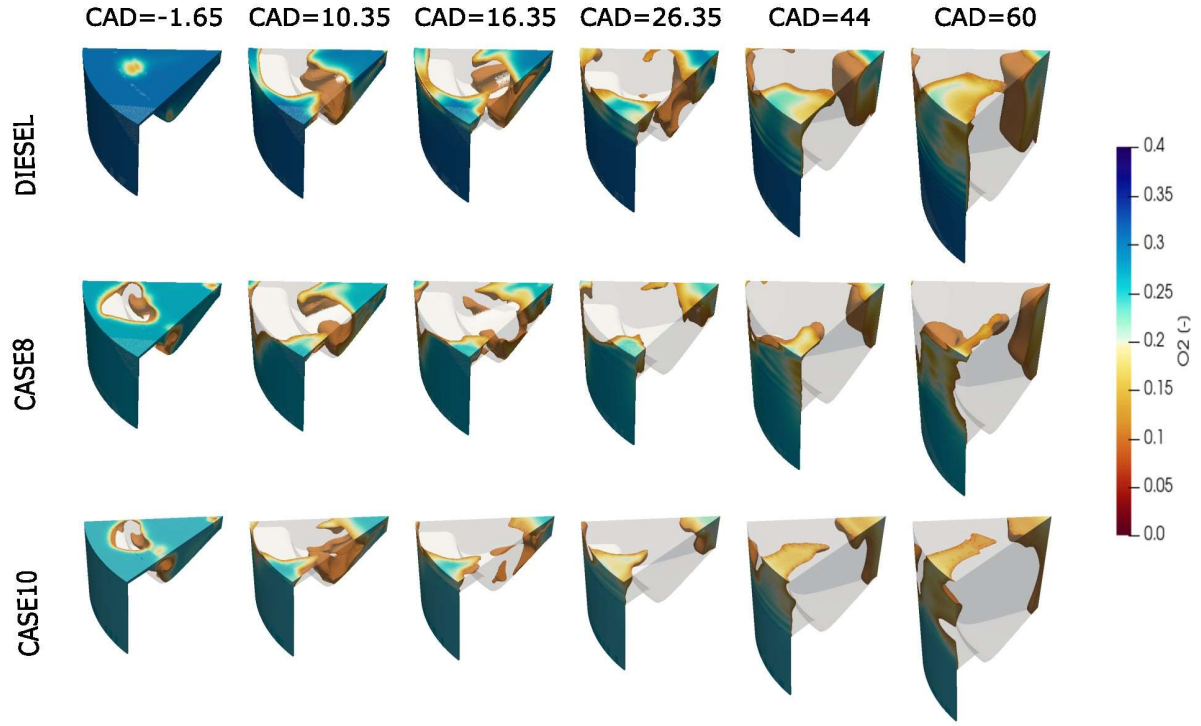

Figure 4.49 Oxygen-content 3D-contours comparison for the final configuration.

In Figure 4.50, more CO_2-content is achieved for 9 holes Y_{IVC}-case since it has a better oxygen utilization and more complete combustion. Resulting in more formation of main combustion products such as CO_2 and H_2O.

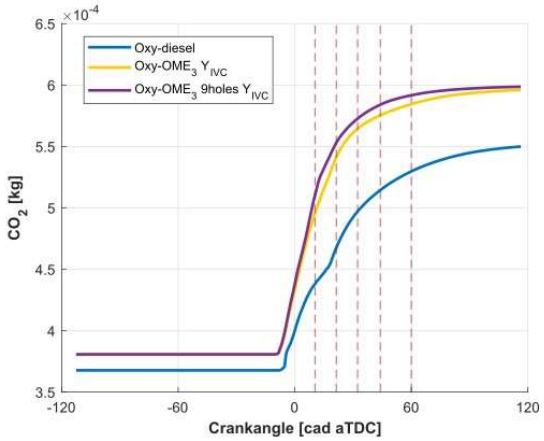

Figure 4.50 Carbon dioxide-content comparison for the study of the final configuration.

The CO2-contours in Figure 4.51 were created with a threshold of 0.45 and over crank angles (-1.65, 10.35, 16.35, 26.35, 44 and 60). The oxy-diesel case has by far the lowest concentrations over all crank angles. At crank angle -1.65 there is no prominent difference between the CO_2-concentrations yet. At higher crank angles clearly the higher CO_2-concentrations are achieved for case 10 (9 holes Y_{IVC}), since there is more dark red shown over larger volumes.

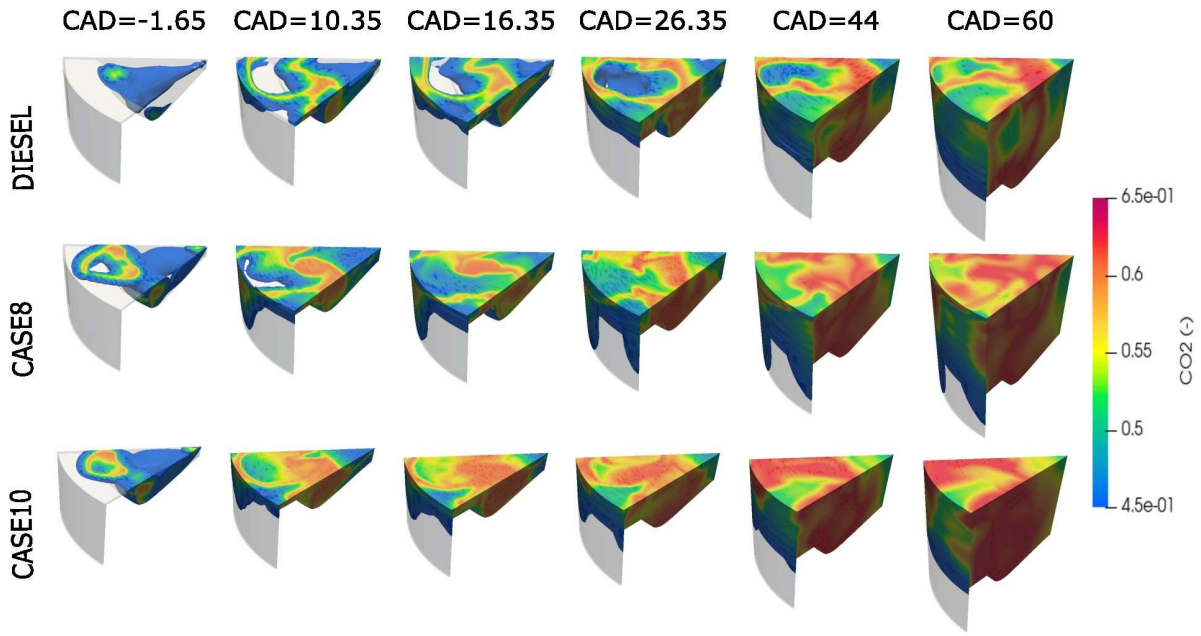

Figure 4.51 Carbon dioxide-content 3D-contours for the final configuration.

In Figure 4.52 the soot precursor C_2H_2 is plotted with the oxy-diesel case excluded since the values for the OME-cases are way smaller. The more complete combustion for the 9 holes Y_{IVC} case results in less formation of C_2H_2 since there are less byproducts formed.

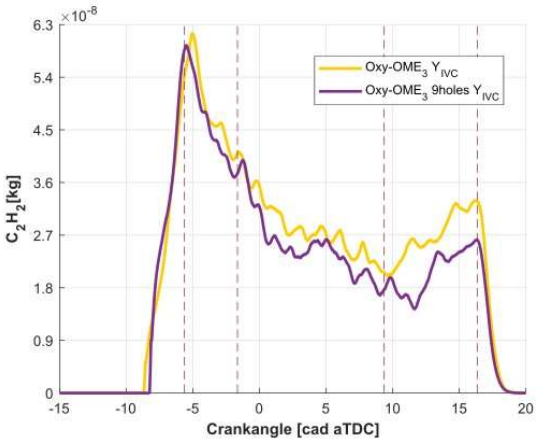

Figure 4.52 Acetylene-content comparison for the study of the final configuration.

In Figure 4.53 the contours of the soot precursor are plotted with a threshold of 1.7e-12 at crank angles (-1.65, 10.35, 16.35, 26.35, 44 and 60) where the same statements as above can be made again. However, here the distribution can be seen, generally the highest C_2H_2-concentrations are at the crevice and the middle of the geometry with little to no concentration in between for the OME-cases.

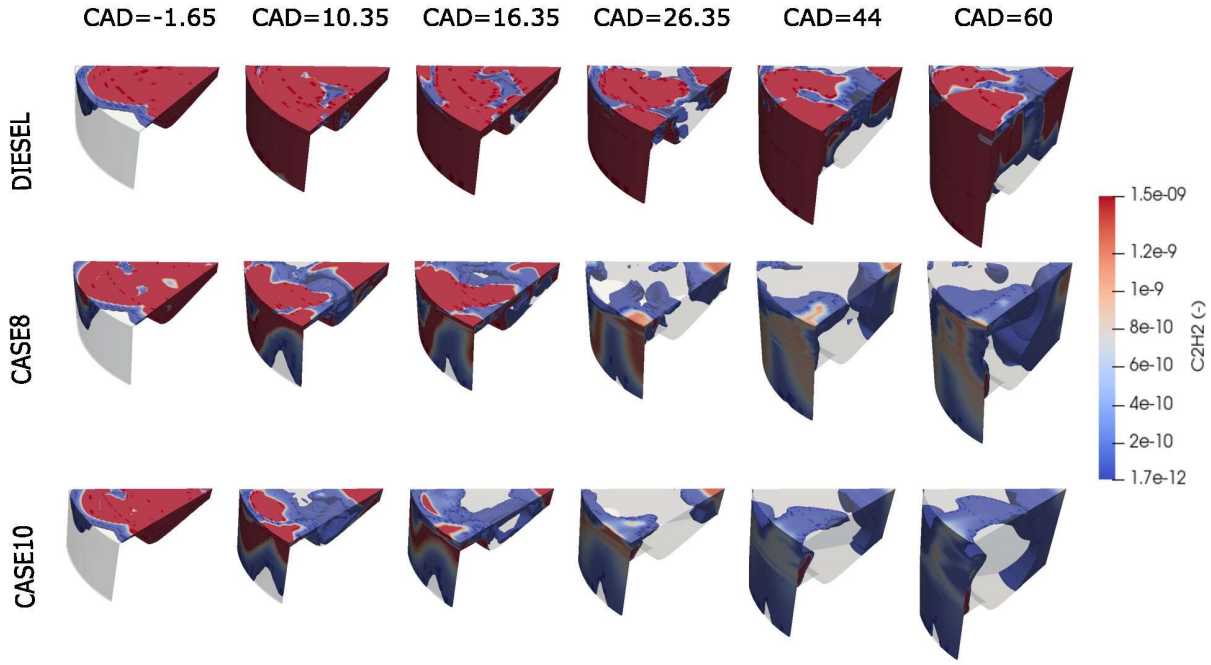

Figure 4.53 Acetylene-content 3D-contours comparison for the final configuration.

Figure 4.54 shows the graphs of the hydroxyl-content. The highest peak of hydroxyl-content is achieved for the 9 holes Y_{IVC}-case. The higher OH-levels come from the more complete combustion resulting in more fuel being burned which leads to more OH-formation since this a normal intermediate product during the reaction. However, the OH-content dips again below the other two graphs since the more complete combustion results in more OH being consumed and reformed to other products.

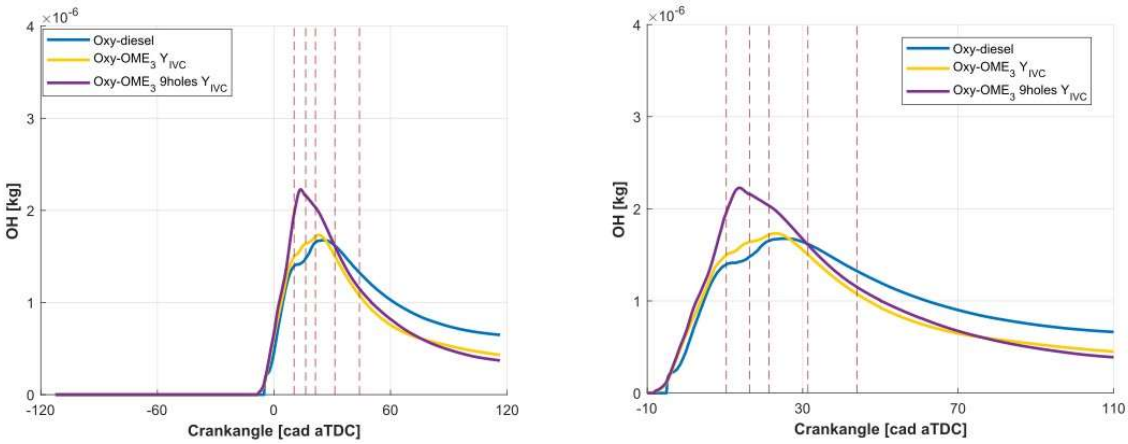

Figure 4.54 Hydroxyl-content comparison for the study of the final configuration.

- **Global engine analysis**

The total cylinder mass distribution is shown in Figure 4.55 over three relevant equivalence ratios. One ratio represents the more stoichiometric condition (mt>1.05), another represent lean condition (mt>0.55) where there is a deficit of fuel and the last one represent rich condition (mt>1.75) where there is an abundance of fuel. The 9 holes Y_{IVC} shows similar behaviour in lean conditions as the Y_{IVC}-case where only the concentrations are changed, although the 9 holes Y_{IVC} case being a bit more lean. However, there is a improvement in mixing rate for the 9 holes Y_{IVC} case at stoichiometric conditions, the mass is consumed faster. The trend between both OME-cases in rich conditions is quite similar. The better mixing rate and faster consumption of mass is due to the reasons mentioned already (improvements in atomization and evaporation due to smaller fuel droplets).

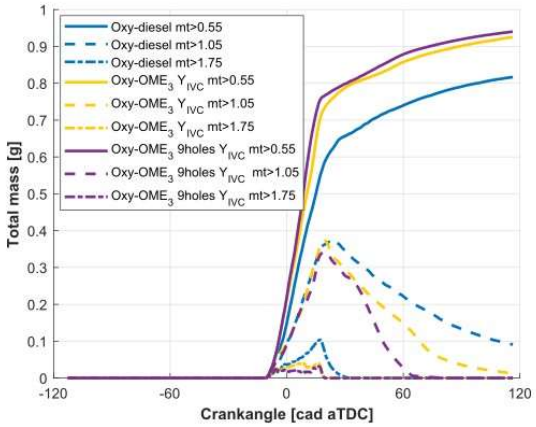

Figure 4.55 Total cylinder mass distribution comparison for the study of the final configuration.

In Figure 4.56 the contours for the mixture fraction are plotted at crank angles (-1.65, 10.35, 16.35, 26.35, 44, 60). The fuel jets at -1.65 are nearly identical for both OME-cases with a bit smaller fuel jet for case 10 (9 holes Y_{IVC}), this is due to the smaller nozzle orifice diameter that tend to provide smaller fuel droplets and the fuel being spread over more injector holes. Moving to crank angle 16.35 again a smaller fuel rich core can be seen as in the number of injector holes comparison. In general over the crank angles 26.35, 44 and 60 less blue is seen in the middle of the geometry and less yellow is seen at

the crevice for case 10 compared to case 8. This shows the better mixing of the fuel with air over the whole geometry.

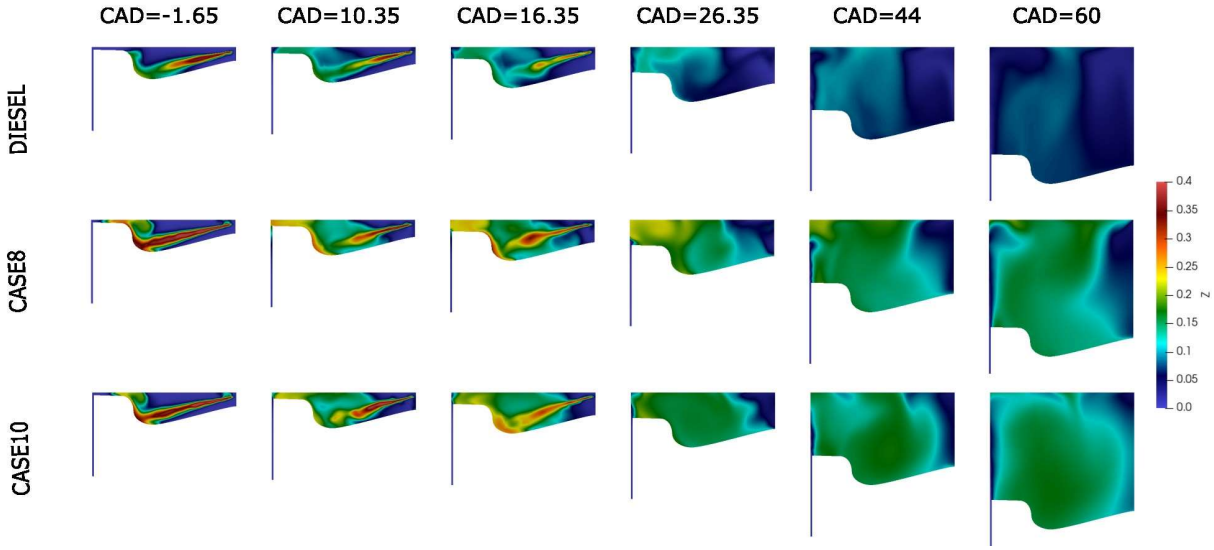

Figure 4.56 Mixture-fraction 2D-contour for the final configuration.

In Figure 4.57 the equivalence ratio in function of temperature is plotted for the three cases in three different graphs. Again we will focus on the case with 9 injector holes and adapted concentrations, the points are being a little more concentrated at the higher temperatures than for the Y_{IVC} case because of the higher peak in-cylinder temperature reached. And at the lower crank angles (CA0 and CA5) the points exceed the NOx limit less because of the better combustion. Exactly the same amount seem to exceed the soot limit for both OME-cases.

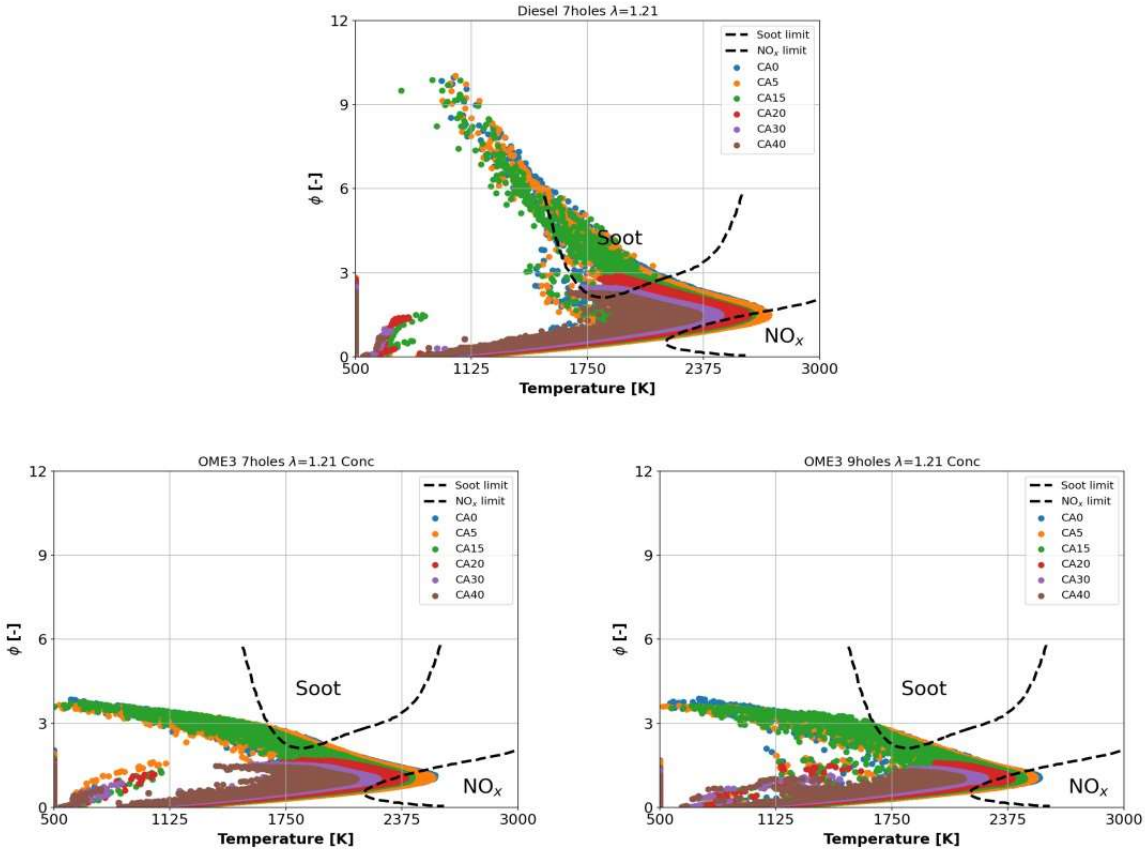

Figure 4.57 Equivalence ratio in function of temperature plot for the 9holes and Y_{IVC} case.

As shown in the results part of the Iso-lambda comparison in section 4.1.2 a worse efficiency was achieved in both cases than diesel, while in the previous comparison we received a better efficiency when rising the amount of nozzle orifices. So here was an attempt to still receive a better efficiency although using a lower lambda value. The better atomization and evaporation of the case with 9 holes again has a positive influence on the combustion process and the 9 holes Y_{IVC} case reaches the highest combustion efficiency in Figure 4.58.

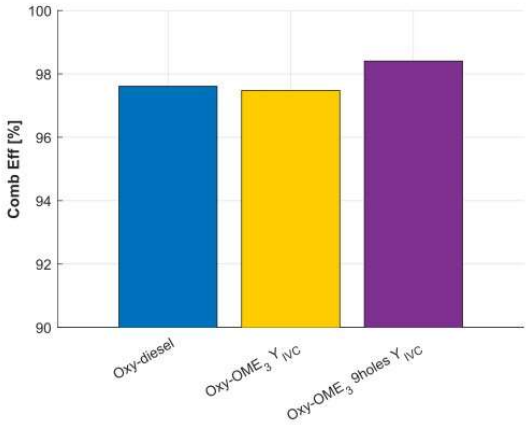

Figure 4.58 Bar-chart of the combustion efficiency for the study of the final configuration.

The influence on the pollutants can been seen in Figure 4.59 below. In the top left corner a decrease in hydrocarbon content is shown if we introduce the 9 injector hole orifices, while still being higher than the oxy-diesel case. There are less unburned hydrocarbons because of the better mixing for the 9 holes Y_{IVC} case compared to the Y_{IVC} case. In the bottom left corner the negligible amount of soot is achieved because of the lack in carbon-carbon bonds. For the hydroxyl content in the top right corner the lowest amount of hydroxyl-content at the end of combustion is achieved for the 9 holes Y_{IVC} case, while the diesel case having by far the highest content. The hydroxyl-content of the diesel case still has to be confirmed with the experiments. In the bottom right corner, a big decrease in carbon monoxide can be seen for the new configuration since it is more completely combusted into CO_2.

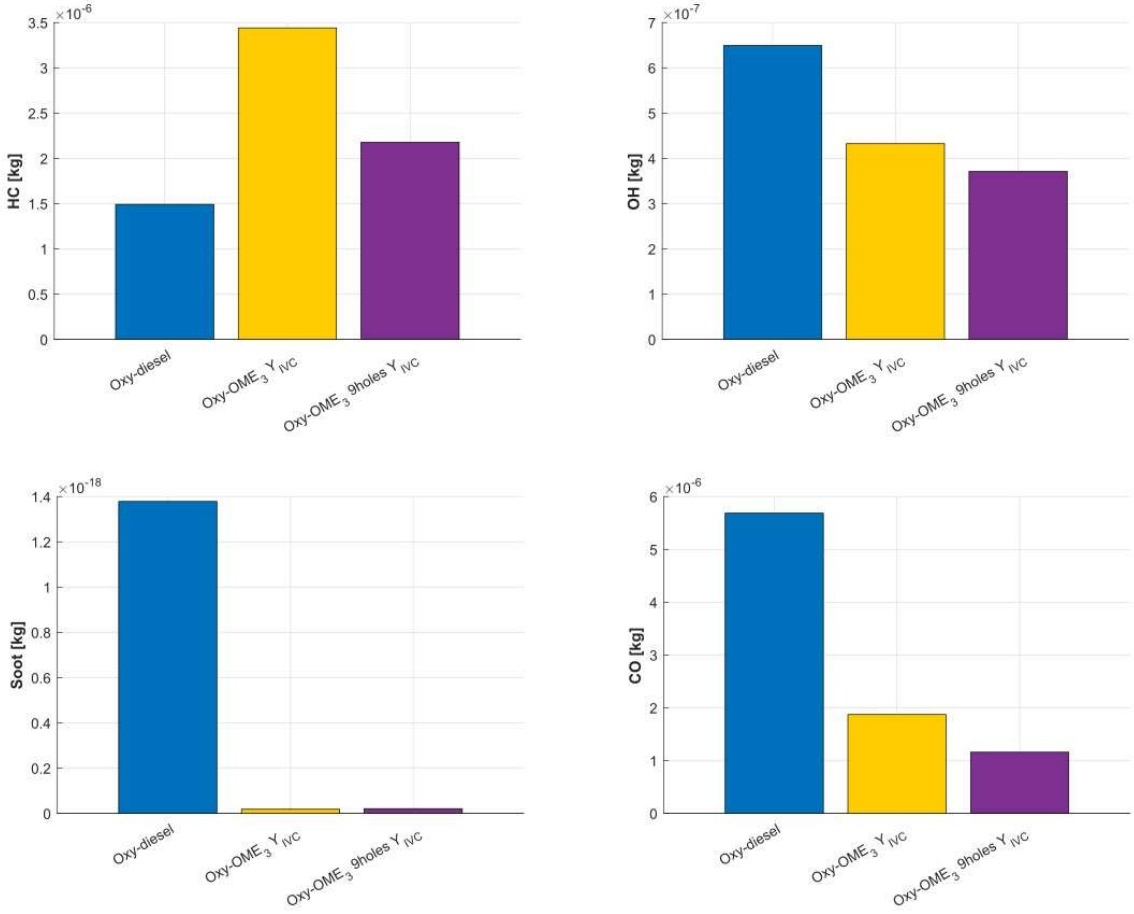

Figure 4.59 Bar-chart of the pollutants for the study of the final configuration.

The bar charts for the indicated mean pressure in Figure 4.60 show a slightly improved fuel economy for the 9 holes Y_{IVC} case than for the case where only the concentrations were changed because of the better combustion efficiency, but still the fuel economy seems to keep being a concern because of the lower LHV. In indicated specific mean pressure there is a slight increase because of the higher peak pressure. [50]

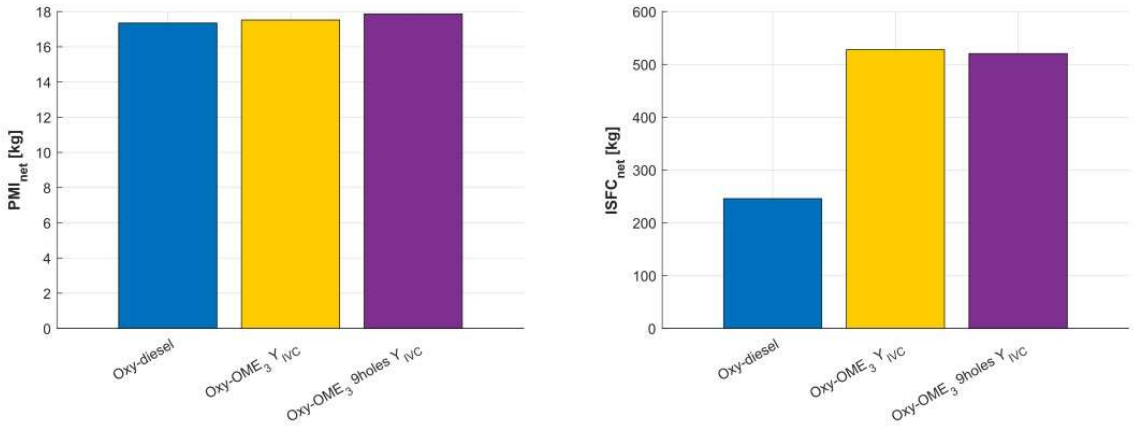

Figure 4.60 Bar-chart of the indicated mean pressure and the indicated specific fuel consumption for the study of the final configuration.

4.3.2 Conclusion for the final configuration

The final configuration seems to be the most favourable since a better combustion efficiency is achieved while working at the same lambda value as diesel and having no soot emissions. Also, the decrease in OH and CO-emissions is very good news. Although, the increase in HC and CO_2-emissions have to be considered as well as the higher values of indicated specific fuel consumption. That is why as previously mentioned much research is still needed to decrease the amount of hydro carbon emissions and to find a way to retrieve a better fuel economy.

5 CONCLUSION

During this analysis, the favourable properties of OME-fuel were analysed to find an alternative to diesel fuel and the emissions it entails. This was done using 3 comparisons where thermodynamic parameters and emissions were considered and then a global engine analysis was compiled. From the first 2 comparisons, we arrived at a most favourable OME case. Namely, from the number of holes comparison, this was case 7 with 9 injector nozzle orifices. While for the iso-lambda comparison, this was case 8 (Y_{IVC}) with the adjusted concentrations. These two cases were then combined to generate a final configuration for this. Here, this configuration came out most favourable in a comparison with the reference diesel case and case 8 (Y_{IVC}). In conclusion, this analysis shows the promising potential of using oxygenated fuels as an alternative to diesel fuel. The research finds that with the right adjustments and further research, these fuels hold a significant promise for the future. However, more extensive research is needed to fully understand what changing other parameters would have on the combustion system and to fully understand the characteristics of OME_3. Since, there is not much extensive research on this yet, it was difficult to back up your results with previous studies and sources. The results show the positive contribution in regards to lower emissions and improved combustion efficiency. But investigating other OME fuels might be a good approach to come to the ideal fuel. Also, looking at blends of different OME-fuels or a blend of diesel and OME might even have better characteristics in terms of emissions, combustion efficiency and fuel economy. Another good approach for the future could be to further look at the design of the engine or operating conditions to make it the most suitable for these kind of fuels.

6 BIBLIOGRAPHIC REFERENCES

[1] "OpenFOAM." https://www.openfoam.com/ (accessed Jun. 13, 2023).

[2] "ParaView - Wikipedia." https://en.wikipedia.org/wiki/ParaView (accessed Jun. 13, 2023).

[3] "About ParaView." https://www.paraview.org/about/ (accessed Jun. 13, 2023).

[4] "What Are Diesel Engines and How Do They Work? - Top One Power." https://www.topone-power.com/info/what-are-diesel-engines-and-how-do-they-work/ (accessed Jun. 13, 2023).

[5] "Internal combustion engine - Wikipedia." https://en.wikipedia.org/wiki/Internal_combustion_engine (accessed Jun. 13, 2023).

[6] "Main parameters of an engine piston and cylinder – x-engineer.org." https://x-engineer.org/engine-piston-cylinder-parameters/ (accessed Jun. 13, 2023).

[7] A. Reddy, "Effect Of Compression Ratio On The Performance Of Diesel Engine At Different Loads," 2015. [Online]. Available: www.ijera.com

[8] P. C. Miles and I. Ö. Andersson, "A review of design considerations for light-duty diesel combustion systems Überblick über Designüberlegungen zum Brennverfahren von PKW-Dieselmotoren," 2015.

[9] J. P. Holman *et al.*, "McGraw-Hill Series in Mechanical Engineering INTERNAL COMBUSTION ENGINE Xnderung nur iiber," 1988.

[10] "4 Stages of combustion in CI engine," 2020. https://www.enggstudy.com/stages-of-combustion-in-ci-engine/ (accessed Jun. 27, 2023).

[11] M. Sebok, M. Gutten, D. Korenciak, M. Bartłomiejczyk, M. Šebök, and D. Korenčiak, "Analysis of pressure ratio in the intake in dependence on high-voltage behaviours Economic-spatial aspects of functioning of the automotive market on example of the production of public transport vehicles View project TROLLEY View project Analysis of pressure ratio in the intake in dependence on high-voltage behaviours", [Online]. Available: https://www.researchgate.net/publication/286368594

[12] S. Bürkle *et al.*, "In-Cylinder Temperature Measurements in a Motored IC Engine using TDLAS," *Flow Turbul Combust*, vol. 101, no. 1, pp. 139–159, Jul. 2018, doi: 10.1007/s10494-017-9886-y.

[13] "Mixture fraction - Wikipedia." https://en.wikipedia.org/wiki/Mixture_fraction (accessed Jun. 29, 2023).

[14] "Air–fuel ratio - Wikipedia." https://en.wikipedia.org/wiki/Air%E2%80%93fuel_ratio#Equivalence_ratio (accessed Jun. 29, 2023).

[15] "ISFC full form in Automobile Engineering." https://www.fullformgo.com/term/ISFC (accessed Jun. 30, 2023).

[16] "Heat capacity ratio - Wikipedia." https://en.wikipedia.org/wiki/Heat_capacity_ratio (accessed Jun. 30, 2023).

[17] O. Kastner, F. Atzler, O. Soriano, and A. Weigand, “Multiple small vs single large pilot injections for Diesel engines,” *Institution of Mechanical Engineers - Fuel Systems for IC Engines*, pp. 183–195, Jan. 2012, doi: 10.1533/9780857096043.5.183.

[18] Semin and Abdul Rahim Ismail, “Effect of injector nozzle holes on diesel engine performance,” 2010. [Online]. Available: www.intechopen.com

[19] Charles Lafayette Proctor and Lloyd Van Horn Armstrong, “Diesel engine | Definition, Development, Types, & Facts | Britannica,” 2023. https://www.britannica.com/technology/diesel-engine (accessed Jun. 13, 2023).

[20] Ismet Celikten, “An experimental investigation of the effect of the injection pressure on engine performance and exhaust emission in indirect injection diesel engines _ I Ismet C ß el_ ı ıkten,” pp. 2051–2060, 2003, doi: 10.1016/S1359-4311(03)00171-6.

[21] “What’s the Commotion About Mixture Motion: Swirl and Tumble Explained.” https://www.motortrend.com/how-to/cylinder-head-swirl-and-tumble/ (accessed Jun. 27, 2023).

[22] “Oxy-fuel combustion process - Wikipedia.” https://en.wikipedia.org/wiki/Oxy-fuel_combustion_process (accessed Jun. 13, 2023).

[23] A. Mohammed, J. B. Masurier, A. Elkhazraji, and B. Johansson, “Oxy-Fuel HCCI Combustion in a CFR Engine with Carbon Dioxide as a Thermal Buffer,” in *SAE Technical Papers*, SAE International, Sep. 2019. doi: 10.4271/2019-24-0119.

[24] M. F. Roslan, I. Veza, and M. F. M. Said, “Predictive simulation of single cylinder n-butanol HCCI engine,” in *IOP Conference Series: Materials Science and Engineering*, IOP Publishing Ltd, Jul. 2020. doi: 10.1088/1757-899X/884/1/012099.

[25] Chris Pagliaro, “The Chemistry of the Diesel Engine,” 2013. https://chembloggreen1.wordpress.com/ (accessed Jun. 13, 2023).

[26] A. Holzer and M. Guenthner, “Investigation of the Emission Reduction Potential of HVO-OME Fuel Blends in a Single-Cylinder Diesel Engine,” 2021.

[27] J. Burger and H. Hasse, “Processes for the production of OME fuels,” 2020, pp. 191–203. doi: 10.1007/978-3-658-30500-0_12.

[28] J. M. García-Oliver, R. Novella, C. Micó, and D. De Leon-Ceriani, “Numerical analysis of the combustion process of oxymethylene ethers as low-carbon fuels for compression ignition engines,” *International Journal of Engine Research*, May 2022, doi: 10.1177/14680874221113749.

[29] J. Burger and H. Hasse, “Processes for the production of OME fuels,” 2020, pp. 191–203. doi: 10.1007/978-3-658-30500-0_12.

[30] M. Drexler, P. Haltenort, T. A. Zevaco, U. Arnold, and J. Sauer, “Synthesis of tailored oxymethylene ether (OME) fuels via transacetalization reactions,” *Sustain Energy Fuels*, vol. 5, no. 17, pp. 4311–4326, Aug. 2021, doi: 10.1039/D1SE00631B.

[31] R. Schmitz, M. Sirignano, C. Hasse, and F. Ferraro, “Numerical Investigation on the Effect of the Oxymethylene Ether-3 (OME3) Blending Ratio in Premixed Sooting Ethylene Flames,” *Front Mech Eng*, vol. 7, p. 744172, Aug. 2021, doi: 10.3389/FMECH.2021.744172/BIBTEX.

[32] “SA Oil | The Difference Between Oxygenated & Unoxygenated Fuel | Race Fuels | SA Oil,” 2018. https://saoil.co.za/oxygenated-vs-unoxygenated-fuel/ (accessed Jun. 13, 2023).

[33] “Cetane number - Wikipedia.” https://en.wikipedia.org/wiki/Cetane_number (accessed Jun. 27, 2023).

[34] Yixuan Wu, Isabelle Ays, and Marcus Geimer, “Analysis and Preliminary Design of Oxymethylene ether (OME) Driven Mobile Machines,” 2019.

[35] B. Kibbe, “Microsoft Word - Lambda as a Diagnostic Tool.doc,” 2007.

[36] “Carbon monoxide - Wikipedia.” https://en.wikipedia.org/wiki/Carbon_monoxide (accessed Jul. 04, 2023).

[37] P. D. Jadhav and J. M. Mallikarjuna, “Effect of fuel injector hole diameter and injection timing on the mixture formation in a GDI engine - A CFD study,” *International Journal of Computational Methods and Experimental Measurements*, vol. 6, no. 4, pp. 737–748, 2018, doi: 10.2495/CMEM-V6-N4-737-748.

[38] S. Martínez-Martínez, F. A. Sánchez-Cruz, J. M. Riesco-Ávila, A. Gallegos-Muñoz, and S. M. Aceves, “Liquid penetration length in direct diesel fuel injection,” *Appl Therm Eng*, vol. 28, no. 14–15, pp. 1756–1762, Oct. 2008, doi: 10.1016/j.applthermaleng.2007.11.006.

[39] M. A. Ceviz and I. Kaymaz, “Temperature and air-fuel ratio dependent specific heat ratio functions for lean burned and unburned mixture,” *Energy Convers Manag*, vol. 46, no. 15–16, pp. 2387–2404, Sep. 2005, doi: 10.1016/j.enconman.2004.12.009.

[40] N. Keerthi Kumar *et al.*, “Effect of Parameters Behavior of Simarouba Methyl Ester Operated Diesel Engine,” *Energies 2021, Vol. 14, Page 4973*, vol. 14, no. 16, p. 4973, Aug. 2021, doi: 10.3390/EN14164973.

[41] D. Mentes, Z. Sajti, T. L. Koós, and C. Póliska, “Optimizing the combustion processes of a small scale solid fuel-fired boiler,” *International Journal of Engineering and Management Sciences*, vol. 4, no. 4, pp. 358–369, Dec. 2019, doi: 10.21791/IJEMS.2019.4.41.

[42] A. Ridhuan, S. A. Osman, M. Fawzi, A. J. Alimin, and S. A. Osman, “A Review of Comparative Study on The Effect of Hydroxyl Gas in Internal Combustion Engine (ICE) On Engine Performance and Exhaust Emission,” *Journal of Advanced Research in Fluid Mechanics and Thermal Sciences*, vol. 87, no. 2, pp. 1–16, Nov. 2021, doi: 10.37934/arfmts.87.2.116.

[43] P. Benjumea, J. R. Agudelo, and A. F. Agudelo, “Effect of the degree of unsaturation of biodiesel fuels on engine performance, combustion characteristics, and emissions,” *Energy and Fuels*, vol. 25, no. 1, pp. 77–85, Jan. 2011, doi: 10.1021/ef101096x.

[44] F. M. Ghanim, A. M. Hamdan Adam, and H. Farouk, “Performance and Emission Characteristics of a Diesel Engine Fueled by Biodiesel-Ethanol-Diesel Fuel Blends,” *International Journal of Advanced Thermofluid Research*, vol. 4, no. 1, pp. 26–36, Jun. 2018, doi: 10.51141/IJATR.2018.4.1.2.

[45] S. Yoon, S. Lee, H. Kwon, J. Lee, and S. Park, “Effects of the swirl ratio and injector hole number on the combustion and emission characteristics of a light duty diesel engine,” *Appl Therm Eng*, vol. 142, pp. 68–78, Sep. 2018, doi: 10.1016/J.APPLTHERMALENG.2018.06.076.

[46] J. Benajes, R. Novella, J. Gomez-Soriano, P. J. Martinez-Hernandiz, C. Libert, and M. Dabiri, “Evaluation of the passive pre-chamber ignition concept for future high compression ratio turbocharged spark-ignition engines,” *Appl Energy*, vol. 248, pp. 576–588, Aug. 2019, doi: 10.1016/j.apenergy.2019.04.131.

[47] C. Dueso *et al.*, “Performance and emissions of a diesel engine using sunflower biodiesel with a renewable antioxidant additive from bio-oil,” *Fuel*, vol. 234, pp. 276–285, Dec. 2018, doi: 10.1016/j.fuel.2018.07.013.

[48] S. SARIKOÇ, “Impact of various lambda values on engine performance, combustion and emissions of a SI engine fueled with methanol-gasoline blends at full engine load,” *International Journal of Automotive Engineering and Technologies*, vol. 9, no. 4, pp. 178–189, Dec. 2020, doi: 10.18245/ijaet.735553.

[49] C. Saupe and F. Atzler, “Potentials of oxymethylene-dimethyl-ether in diesel engine combustion,” *Automotive and Engine Technology*, vol. 7, no. 3–4, pp. 331–342, Dec. 2022, doi: 10.1007/s41104-022-00117-5.

[50] A. García, A. Gil, J. Monsalve-Serrano, and R. Lago Sari, “OMEx-diesel blends as high reactivity fuel for ultra-low NOx and soot emissions in the dual-mode dual-fuel combustion strategy,” *Fuel*, vol. 275, Sep. 2020, doi: 10.1016/j.fuel.2020.117898.

[51] J. J. Cano-Gómez, G. A. Iglesias-Silva, P. Rivas, C. O. Díaz-Ovalle, and F. De Jesús Cerino-Córdova, “Densities and Viscosities for Binary Liquid Mixtures of Biodiesel + 1-Butanol, + Isobutyl Alcohol, or + 2-Butanol from 293.15 to 333.15 K at 0.1 MPa,” *J Chem Eng Data*, vol. 62, no. 10, pp. 3391–3400, Oct. 2017, doi: 10.1021/ACS.JCED.7B00440/ASSET/IMAGES/MEDIUM/JE-2017-00440S_0005.GIF.

BUDGET

7 BUDGET

The last part of this exposition of this project consists of an estimate of the total cost of this project. This incorporates hourly costs, equipment costs and also the cost of licences for the various software's. Knowing these costs is important in order to get future insights into the costs of similar projects. The costs have been divided over a period of 5 months since this is the time there has been worked on the project described in this report. Also, the VAT rate has to be considered, Spain has a general VAT rate of 21% and this will be taken into account at the end of the calculations. Furthermore, for each part a complementary cost of 5% is taken into account as there will be an inaccuracy on the estimations. Moreover, a percentage of 16% will be added to compensate for the indirect costs that this project contains.

7.1 Equipment costs

For the work on the project, a desktop computer was obtained from the "Instituto Universitario de Motores Térmicos CMT. A purchase price of 800 euro was assumed with an amortisation time of 5 years this suggests a monthly cost of 13.34€/ month. For the Matlab Student license the full amount of license was taken into account.

Table 6 Estimation of the equipment costs

	Cost (€)	Usage	Subtotal (€)
Desktop computer	13.34/month	5 months	66.7
Paraview license	0/year	/	0
Matlab Student license	69/year	/	69
OpenFOAM subscription	0/year	/	0
Internet access	30/month	5 months	600
Complementary cost (5%)			36,79
		Total (€)	772,49

7.2 Human resources

The dedicated time of the student has been based on the amount of hours one ECTS credit needs, this is around 25 hours. The TFM consists out of 20 ECTS-credits resulting in a dedicated time of 500 hours. The project was also guided by a supervisor and a co-supervisor, their hours have been taken into account too. The hourly rates were achieved from a paper received from my supervisor where an increase of 15% was taken into account because of the rise in wages.

Table 7 Estimation of the human resources costs

	Salary (€/h)	Dedicated time (h)	Subtotal (€)
Student	4.5	500	2250
Computer technician	15.00	5	75
Supervisor	30.00	40	1200
Co-supervisor	30.00	70	2100
Complementary cost (5%)			281.25
		Total (€)	**5906.25**

7.3 Total project cost

Table 8 Estimation of the total cost of the project

	Cost (€)
Equipment cost	772.49
Human resources	5906.25
Material execution budget	6678.74
General cost (16%)	1068.60
Contract execution budget	7747.34
VAT (21%)	1626.94
Tender base budget	**9374.31**

The present budget comes to the said amount of:

NINE THOUSAND THREE HUNDRED AND SEVENTY-FOUR EURO AND THIRTY-ONE CENTS

ESCOLA TECNICA SUPERIOR ENGINYERIA INDUSTRIAL VALENCIA
UNIVERSITAT POLITECNICA DE VALENCIA
Camí de Vera s/n – Edificio 5F
46022 VALÈNCIA, España
tel. + 34 963 87 71 70
informatica@etsii.upv.es
https://www.etsii.upv.es/